Max Planck Institute
for Chemical Ecology

Friedrich-Schiller-Universität Jena
Biologisch-Pharmazeutische Fakultät

Diploma Thesis

Characterization of inhibitory olfactory projection neurons in *Drosophila melanogaster*

Submitted by
Amelie Baschwitz
[October/06/2011]

First Reviewer: Prof. Dr. Bill S. Hansson

Second Reviewer: PD Dr. Dieter Wicher

Table of Contents

1. Introduction

The aim of this work was the analyses of a subset of projection neurons (PNs) within the olfactory circuitry of the fruit fly *Drosophila melanogaster,* which is putatively inhibitory (Okada *et al.*, 2009). Since most PNs that have been analyzed so far are cholinergic and thus excitatory, it is necessary for the understanding of the neural circuitry within the antennal lobe (AL) and higher olfactory processing centers to analyze the role and function of these inhibitory PNs. Therefore, I used for morphological analyses the genetic tools provided by the GAL4-UAS system (Brand & Perrimon, 1993) as well as the potentiality of photoactivatable green fluorescent protein (PA-GFP; Patterson & Lippincott-Schwarz, 2002) that enables labeling of single neurons by photoactivation. The labeling of all neurons of interest of the enhancer trap line MZ699 in living flies allowed me to further analyze their innervation pattern in the entire brain. Furthermore, in order to determine the functional role of these neurons I verified the type of expressed neurotransmitter in these PNs by using immunostaining in dissected fly brains against the inhibitory neurotransmitter γ-aminobutyric acid (GABA) and against the enzyme choline acetyltransferase (ChAT), which is producing the excitatory neurotransmitter acetylcholine (ACh).

1.1 Olfaction in *Drosophila*

During their life time animals - and in this context of special interest the fruit fly - are surrounded by a great variety of odors. For an animal it is vital to perceive odors since they indicate food sources, danger, good mates and oviposition sites. The olfactory system has therefore been developed in a way to achieve high sensitivity and best distinctness. Since the olfactory systems of insects and higher animals show remarkably analogy in their functional organization (Hildebrand & Shepherd, 1997) it is appropriate to analyze the olfactory system in the fruit fly. Advantages using the model-organism *Drosophila* including short reproduction cycle, easy breeding, a mass variety of genetic tools (see review Luo *et al.,* 2008), and the complete sequenced genome (Adams *et al.*, 2000) delivered insight into the function of olfaction even on molecular basis. However, the interaction of all players within the olfactory system remains still unclear (see reviews by e.g. Liang & Luo, 2010; Hansson *et al.*, 2010; Su *et al.*, 2009; Stocker, 1994).

1.2 Neural circuitry in the *Drosophila* olfactory system

The olfactory organs on the fore-head of the fruit fly are the maxillary palps and the antennae, especially the third antennal segment, the so-called funiculus. Different types of sensilla (basiconic, coeloconic, trichoid sensilla) cover the surface of these organs: about 420 olfactory sensilla on each antenna and about 60 olfactory sensilla on the maxillary palps are intermingled with non-olfactory sensilla (Fig 1 A). Two to four olfactory sensory neurons (OSNs) housed in the sensilla lie protected in aqueous lymph secreted by supporting cells (Shanbhag *et al.*, 1999). More or less volatile odor molecules get into the sensilla by passing through tiny pores in the sensilla wall (Fig. 1 B). Odorants and pheromones are hydrophobic, so within the lymph they bind to odorant binding proteins (OBPs; Xu *et al.*, 2005) and then attach to different types of odorant receptors (ORs), which are integrated into the cell membrane of the dendrites of OSNs. In *Drosophila* 62 ORs are encoded by 60 OR genes responding to a huge variety of odors (Clyne *et al.*, 1999; Vosshall *et al.*, 1999; Gao & Chess, 1999; Vosshall *et al.*, 2000; Robertson *et al.*, 2003). Apart from the ORs there also exist ionotropic receptors (IRs) that differ in their structure to ORs but also bind odors (Benton *et al.*, 2009). One OR called Orco (formerly Or83b; Vosshall *et al.*, 2000; Larsson *et al.*, 2004) is common in nearly all OSNs along with another one or two ORs (Dobritsa *et al.*, 2003; Larsson *et al.*, 2004; Goldman *et al.*, 2005). The expression of Orco is sufficient for the arrangement of the ORs within the OSN membrane (Benton *et al.*, 2006) and is sufficient for the detection of odors (Larsson *et al.*, 2004). Orco and another OR form a heteromeric receptor ion-channel complex depolarizing OSNs after odor binding (ionotropic signaling pathway; Sato *et al*., 2008; Wicher *et al*., 2008). Also a metabotropic signaling pathway is described that OR-binding activates Orco via a G-protein (Wicher *et al*., 2008; Sargsyan *et al*., 2011). Most ORs are expressed in 10 to 40 OSNs (Vosshall *et al.*, 1999). About 1200 OSNs of the antennae project via the antennal nerve, and 100 OSNs of the maxillary palps project via the labial nerve into the antennal lobe (AL), the first olfactory processing center. The majority of OSNs innervate ipsilateral and contralateral both ALs (Stocker *et al.* 1990). The AL consists of distinct structures, so-called glomeruli which have a specific size and position. Each one of the ~ 50 glomeruli is innervated by the same class of OSNs expressing the same OR type (Laissue *et al.*, 1999; Couto *et al.*, 2005; Fishilevich & Vosshall, 2005). A few OSNs innervate two glomeruli in contrast to the common principle of one neuron innervating one glomerulus (Vosshall *et al.*, 2000; Fishilevich & Vosshall, 2005). Within the AL OSNs synapse onto second order neurons, so-called projection neurons (PNs; Fig. 1 C), innervating higher olfactory processing centers like the mushroom bodies (MB) and the lateral horn (LH; also

lateral protocerebrum, LPR). Approximately 150 PNs with their cell bodies located in three different cell clusters (antero-dorsal, lateral, ventral) around the AL innervate one (uniglomerular) or a few glomeruli (multiglomerular). Uniglomerular PNs project via the inner antenno-cerebral tract (iACT) to the calyx and the LH, or they project via the outer ACT (oACT) first to the LH and then to the calyx (Fig 1D). Multiglomerular PNs project via the middle ACT (mACT) directly to the LH and bypass the calyx region. PNs of the anterodorsal and lateral cell cluster are cholinergic and thus excitatory; some ventral PNs are GABAergic (Okada *et al.*, 2009; Jefferis *et al.*, 2007; Wilson & Laurent, 2005). Also in the AL local interneurons (LNs) are connected to OSNs and PNs. LNs modulate the response patterns of these neurons which can result in a broadening of the PN tuning (Wilson *et al.*, 2004) as well as a narrowing of PN responses (Y. Seki, personal communication) in comparison to the OSN responses. LNs innervate almost all glomeruli

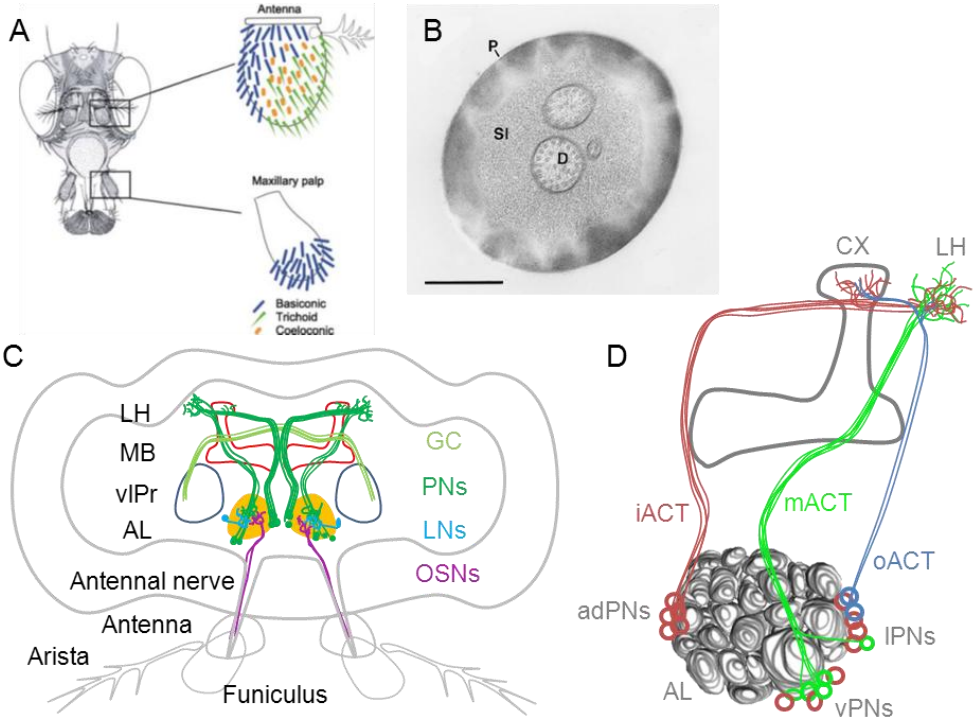

Fig. 1: (A) Scheme of olfactory organs on the head of the fly, and organization of the different sensilla types on the antenna and the maxillary palps (adapted from Liang & Luo 2010). (B) Cross-section through hair shaft of trichoid sensilla with P pores, D unbranched dendrites and Sl sensillar lymph (Shanbhag *et al.*, 1999). (C) Scheme of the olfactory circuit in the fly brain. (D) Cell cluster of the PNs and their projections via different antenno-cerebral tracts to the higher brain centers. adPNs antero-dorsal cell cluster, iACT inner antenno-cerebral tract, lPNs lateral cell cluster, mACT medial antenno-cerebral tract, oACT outer antenno-cerebral tract, vPNs ventral cell cluster. Abbreviations: AL antennal lobe, GC great commissure, MB mushroom body, LH lateral horn, LNs local interneurons, OSNs olfactory sensory neurons, PNs projection neurons, vlPr ventrolateral protocerebrum.

(Seki *et al.*, 2010) and are partly excitatory and cholinergic (Shang *et al.*, 2007), some are glutamatergic (Chou *et al.*, 2010), also peptidergic LNs are described (Ignell *et al.*, 2009); and approximately 100 are inhibitory LNs (iLNs) and release GABA. It is so far still unclear how the odor information is processed by the different neuronal populations within the AL and how this processing leads to an odor perception in higher brain centers which subsequently results in an olfactory behavior.

1.3 Projections of the GAL4-strains GH146 and MZ699

The GH146-GAL4 enhancer trap line, which has been described by Stocker *et al.* (1997), labels mainly uniglomerular projection neurons (PNs; Fig. 2A). These are approximately 100 neurons with their cell bodies in the anterodorsal (~ 50 somata), lateral (~ 40 somata) and ventral (~ 5 - 10 somata) cell clusters around the AL. The glomeruli show a strong innervation pattern by these PNs but a few glomeruli are not innervated at all. Only a subset of 32 glomeruli (about 60%) is innervated by the GH146-GAL4 line (V. Grabe, unpublished). The majority of PNs in the GH146-line projects via the iACT into the LH with arborizations into the calyx. In both regions, the calyx and the LH bulky synaptic terminals are visible. Only a few PNs project via the mACT into the LH bypassing the calyx. The neurites that project via the iACT and mACT sometimes converge before entering the LH. Moreover almost the whole MB shows a strong innervation. A sexual dimorphism of these neurons has not been described so far. I could observe inaddition that the GH146-GAL4 line revealed also a labeling of the dorsal giant interneuron (DGI) with its cell body next to the ventro-lateral protocerebrum (vlPr).

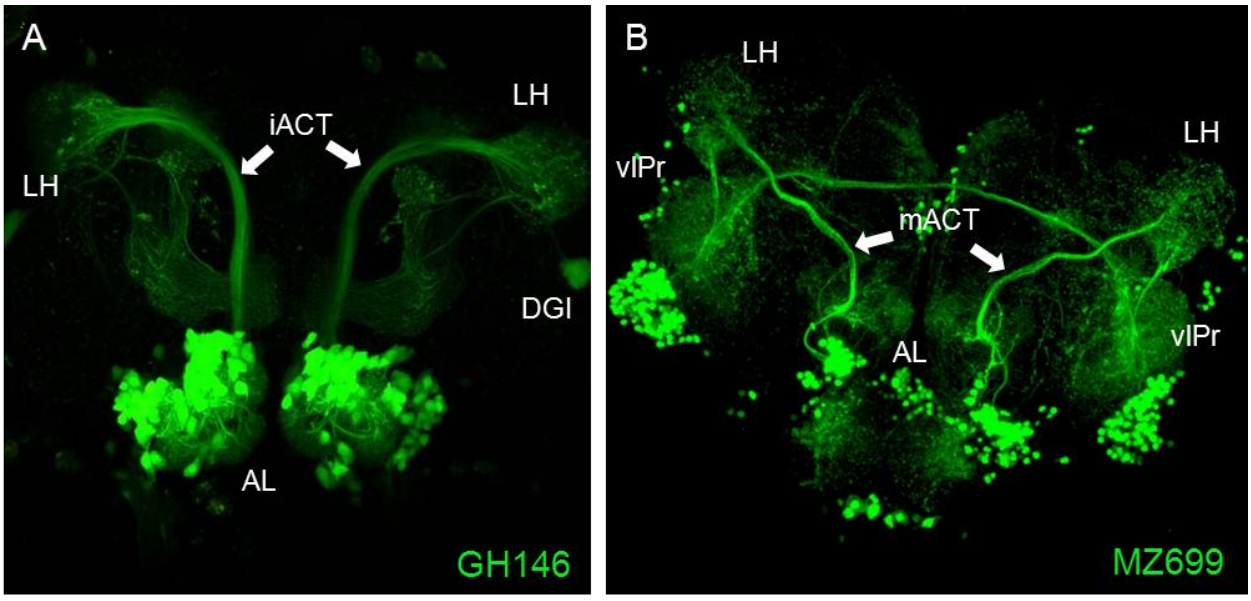

Fig. 2 Images of labeled neurons in the enhancer trap lines GH146 and MZ699 (A and B). Abbreviations: AL antennal lobe; DGI dorsal giant interneuron; iACT inner antenno-cerebral tract; LH lateral horn; mACT medial antenno-cerebral tract; vlPr ventro-lateral protocerebrum.

Besides the GH146-GAL4 line there exists another enhancer trap line that labels a non-overlapping subset of PNs in the fly AL. This line is called MZ699-GAL4 and has been described by Ito *et al.* (1997). Unfortunately, this line does not label only olfactory PNs but also several other neurons in the fly brain (Fig. 2 B). Neurons belonging to that GAL4 line are of the

suboesophageal ganglion (SOG), which are sending fibers via the median bundle (mbdl), cells above the superior protocerebrum (sPr) innervating the sPr via the mbdl, as well as neurons of the ventro-lateral protocerebrum (vlPr), which are interconnected via the great commissure (GC) and innervating the LH. Most interesting for my studies are the olfactory PNs labeled by this line, which are innervating the AL and projecting via the mACT directly into the LH. The somata of these PNs lay in a cluster ventral to the AL next to the cell cluster of neurons innervating the SOG. Approximately 50 neurons of the ventral cell cluster are labeled (Okada *et al.*, 2009; Lai *et al.*, 2008). MZ699-PNs innervate the AL and project directly to the LH via the mACT. These neurons are described to be mainly oligoglomerular (Marin, 2002; Wong *et al.*, 2002), while ~ 1/3 seems to be uniglomerular (Lai *et al.*, 2008). Moreover it is assumed that these PNs are GABAergic and thus inhibitory (Okada et al, 2009). The role of these PNs for odor coding and processing is so far completely unknown since they have not been analyzed in detail.

1.4 Aim of this work

During my diploma thesis I aim to morphologically characterize putative inhibitory PNs in the *Drosophila* olfactory system using the MZ699-GAL4 enhancer trap line.

The MZ699-PNs are presumably inhibitory as Wilson *&* Laurent (2005) showed that PNs of the ventral cell cluster express the inhibitory neurotransmitter GABA. To verify this assumption I will use immunostainings for the identification of the neurotransmitter in this subgroup of PNs. An antibody staining against the inhibitory neurotransmitter GABA will show, if these PNs are indeed GABAergic. Moreover, using an antibody staining against choline acetyltransferase (ChAT), the enzyme producing the excitatory neurotransmitter acetylcholine (ACh), I will verify in a control experiment whether these PNs are cholinergic and thus excitatory.
To analyze the morphology of these PNs in detail I will use photoactivatable green fluorescent protein (PA-GFP; Patterson & Lippincott-Schwarz, 2002), which will be genetically expressed in MZ699-PNs using the GAL4-UAS transcription system (Brand & Perrimon, 1993). PA-GFP (especially C3PA; described by Ruta *et al.*, 2010) can be activated by irradiation with visible or infrared-light and the increase of the fluorescence signal allows subsequent analyses of these illuminated structures. Therefore, I aim to establish a protocol for the photoactivation of this GAL4-line to analyze the innervation patterns of single neurons in different brain areas as the AL and the LH by adapting a protocol which has recently been used for the photoactivation of GH146-PNs (Datta *et al.*, 2008; Ruta *et al.*, 2010). Either the photoactivation of complete brain areas (e.g. AL, LH) or the labeling of subsets of PNs innervating specific glomeruli shall reveal the innervation patterns of these regions. In order to study the PN innervation of glomeruli that have been shown to play a relevant role for the fruit flies' behavior I will photoactivate the glomerulus DA1, which is innervated by OSNs that respond to the so far only known sex pheromone in *Drosophila* (11-*cis*-vaccenyl acetate). Additionally, I will study PNs innervating the VM2-glomerulus, which is activated by odors that are behaviorally attractive (Stökl *et al.*, 2010). In order to identify individual glomeruli in the MZ699-GAL4 line and to define the region of interest for the photoactivation, the generation of an *in vivo* 3D-map of the AL is needed wich represents another part of this diploma thesis. Moreover, I aim to morphologically characterize single PNs by photoactivation of single cell bodies.

2. Material & Methods

2.1 Breeding & Crossing of flies

All fly lines I used were raised at 23 °C with 70 % humidity in an incubator with a 12/12 hour light/dark cycle and flipped every two weeks to a vial with fresh food. One liter of fly food consists of 918 ml water, 95 g polenta, 11 g brewer's yeast, 2.4 ml propionic acid, 3.3 ml nipagine (16%), 118 g sugar beet molasses and 4.1 g agarose.

I used for my experiments different GAL4-enhancer trap fly lines combined with specific UAS-elements established by Brand & Perrimon (1993). This GAL4-UAS transcription system consists of a driver line, composed of an endogenous promoter and the GAL4-sequence, and a responder line, composed of a GAL4 binding site and the target sequence, which initiates the expression of a target sequence. GAL4 is a transcriptional activator (found in the yeast *Saccharomyces cerevisiae*), whose gene could be inserted anywhere into the fly genome provided that there is no endogenous target in the organism. One of a broad range of genomic enhancer can drive the expression of the GAL4 protein in a cell- or tissue-specific pattern. The GAL4 protein binds to the GAL4 binding site called Upstream Activating Sequence (UAS). Several in tandem arranged UAS-elements inserted within the promoter of the gene of interest make it possible to activate the transcription of this gene. This enables to analyze the role of this gene for example in development. Different GAL4- and UAS-elements are usually separated in distinct transgenic fly lines. Crossing of these different lines enables various combinations of expression patterns (reviewed by Elliott & Brand, 2008).

Flies of the genotypes +; GC3.0; MZ699 (provided by A. Strutz) and +; UAS-GFP nls; MZ699 (provided by Y. Seki) were used for the immunostaining. In these fly lines inhibitory PNs (labeled by the MZ699-GAL4 line) express the calcium-sensitive protein GCaMP3.0, a derivative of the green fluorescent protein GFP (Nakai *et al.*, 2001), or GFPnls, which is expressing GFP in the nucleus only, because of the nucleus localization sequence.
For the photoactivation experiments I used flies that have inserted the gene of the photoactivatable GFP (PA-GFP; Patterson & Lippincott-Schwarz, 2002). PA-GFP is a codon-optimized version of the wild-type GFP from the jellyfish *Aequorea Victoria* (reviewed by Van Thor, 2009). An amino acid substitution in the protein decreases the minor absorbance peak, which results in an increase of the fluorescence signal-to-background ratio after photoactivation. PA-GFP has the property that illumination converts the chromophore population resulting in a 100-fold increase

of fluorescence. The photostability of PA-GFP is comparable to GFP (Patterson & Lippincott-Schwarz, 2002). I used the PA-GFP variant called C3PA (Ruta *et al.*, 2010).

Flies of the MZ699-GAL4-line and GH146-GAL4-line were crossed to express UAS-C3PA in different types of PNs. In the GH146-GAL4 line the PNs show a clear glomerular innervation pattern but since the MZ699-enhancer trap line is multiglomerular, identification of single glomeruli is almost impossible. To overcome this problem, the construct END1-2 generated by A. Strutz (unpublished) was combined with the C3PA-flies. END1-2 is a P-element (reviewed by Hummel & Klämbt, 2008) consisting of elav combined to n-synaptobrevin-DsRed1-2. The protein ELAV (embryonic lethal abnormal vision), ubiquitous in *Drosophila melanogaster,* is binding to RNA involved in the development of the central nervous system and thus can be used as a general marker for neurons (reviewed by Yao *et al.*, 1993). The neuronal synaptobrevin (n-syb) is a synaptic vesicle protein expressed in the *Drosophila* nervous system (DiAntonio *et al.*, 1993) and enables specific labeling of presynapses. DsRed is a kind of red fluorescent protein found in the coral *Discosoma striata* (Matz *et al.*, 1999). To assemble this construct a pCaST-elav-Gal4AD vector (plasmid 15307; addgene, Cambridge, MA) was used. The GAL4 activation domain (Gal4AD) was cleaved at the restriction sites Not1 and FspA1 by Addgene. The FspA1 site is within the DsRed coding sequence. Hence, a modified sequence of n-syb (DiAntonio *et al.*, 1993), with an amino acid substitution of arginine instead of alanine to abscise the FspA1 site and a removed stop codon of n-syb, has been synthesized and ligated by Eurofins MWG GmbH (Ebersberg, Germany). This modified n-syb contained also a *Drosophila* Kozak sequence (cAAaATG) after the elav-promoter to increase translation rates (Cavener, 1987). This vector was amplified in *Escherichia coli* (One Shot® Top10 *E. coli*, Invitrogen, Eugene, OR) and the purified vector was injected into *Drosophila* w1118 embryos (Aktogen Ltd., Cambridge, UK), which have a mutation in the *white* gene and show a white eye color instead of red. Hatched transgenic flies show orange to red eyes, because the *mini-white* gene inserted in the vector is translated and the protein for the eye pigment is expressed. The other ones with white eyes have no vector inserted (Bachmann & Knust, 2008). The END1-2 construct I used is located on the second chromosome. Flies with END1-2 expression show red fluorescence of DsRed in presynapses resulting in a staining of the neuropil (Fig. 3). Due to the fact that DsRed underlies photobleaching, END1-2 has to be homozygous for an increased expression of DsRed. In my analyses I used flies having the UAS-element C3PA and the END1-2 construct on the second chromosome, as well as MZ699-GAL4 on the third chromosome. All of these genes had to be homozygous for a high expression of C3PA and DsRed. Therefore a recombination of the

END1-2 and the C3PA on the second chromosome was necessary (Fig. 4). Finally, I used 1 to 7 days old female flies of the genotypes +; GH146; C3PA and +; END1-2,C3PA; MZ699 for the photoactivation experiments.

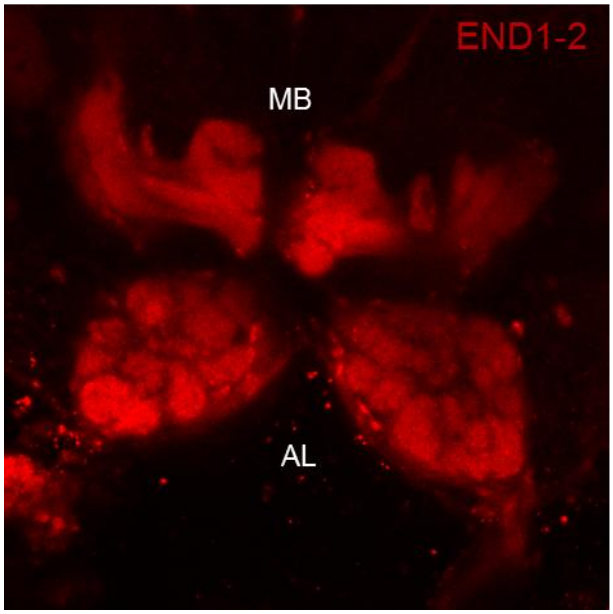

Fig. 3 (left): Flies with the END1-2 construct show red fluorescence staining in the neuropil. AL antennal lobe, MB mushroom body.

Fig. 4 (down): Crossing and recombination of the used fly lines. (P) Flies having these genotypes were crossed to recombine both END1-2 and C3PA on one chromosome. (F1) Female flies of this genotype were crossed with double-balancer (DB) males. (F2) In the second filial generation male flies with red eyes and curly wings (CyO) have on the second chromosome a recombination of END1-2 and C3PA; they were crossed with female flies of the MZ699-GAL4 line. Those flies with orange eyes have either C3PA or END1-2; flies with white eyes have no insertion. (F3) Flies with all three insertions were crossed with each other to get homozygous flies for the photoactivation experiments.

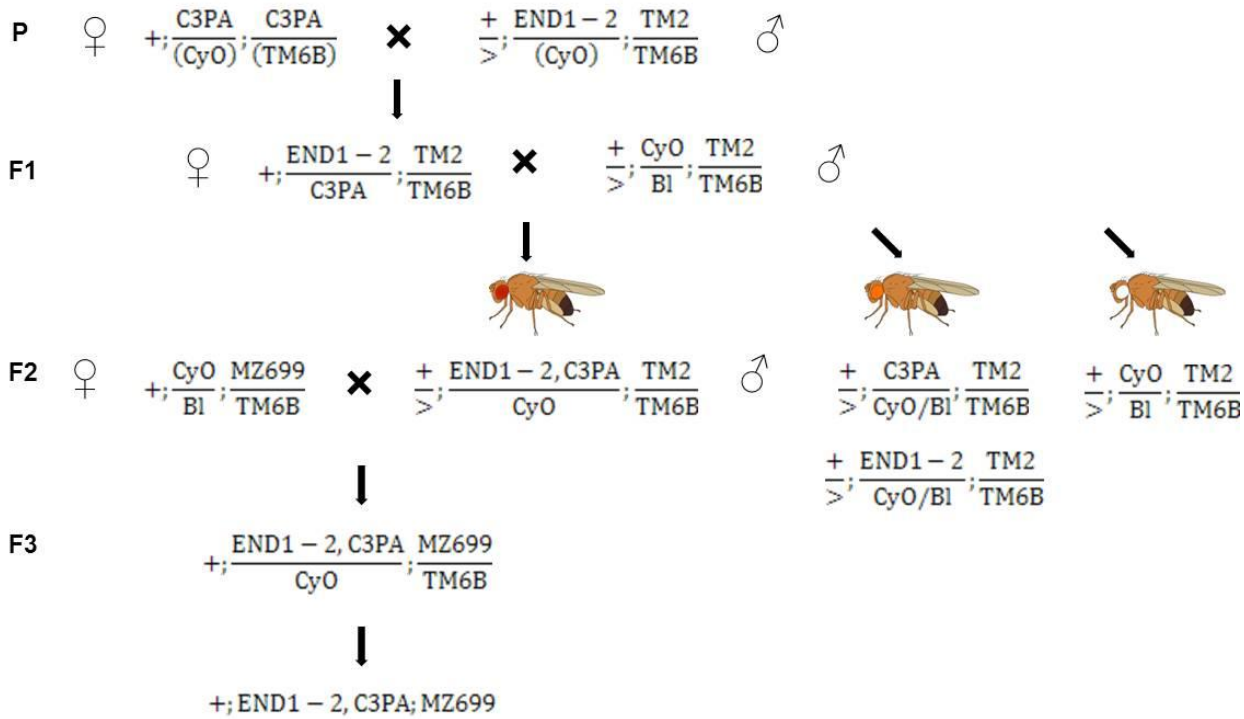

2.2 Immunostaining

For the analyses of the presumably inhibitory PNs, which are labeled by the enhancer trap line MZ699, I used immunostaining to check, if the PNs express the inhibitory neurotransmitter γ-aminobutyric acid (GABA). To show that they also do not express the excitatory neurotransmitter acetylcholine (ACh) further immnunostainings were made using an antibody against the enzyme choline acetyltransferase (ChAT), the producing enzyme of ACh. Female flies of the genotypes +; GC3.0; MZ699 (A. Strutz) and +; UAS-GFP nls; MZ699 (Y. Seki) aged between 1 to 6 days after hatching were used. To analyze age-specific differences female flies with an age of a few hours after eclosion and up to 15 days were prepared as following:

The flies were anesthetized by placing the vial for at least 10 min on ice. Fly brains were dissected and stained as described in Wu & Luo (2006) except for some variations. I dissected the fly brains in *Drosophila* Ringer solution (NaCl 7.6 g/l, KCl 0.37 g/l, $MgCl_2$ $6H_2O$ 0.41 g/l; $CaCl_2$ 2 H_2O 0.29 g/l; saccharose 12.32 g/l; HEPES 1.19 g/l; pH 7.3) in a petri dish. To increase the penetration of the antibodies into the tissue the neurilemma was removed. The brains were transferred with fine forceps to a tube also filled with *Drosophila* Ringer solution. After the brains have settled to bottom the solution was replaced by 4% paraformaldehyde (PFA) in phosphate-buffered solution (PB; 0.1M, pH 7.4) for a 30-min fixation on ice. The PFA-solution was replaced by phosphate-buffered solution (PB; 0.1M, pH 7.4) containing 0.2% Triton X-100 (PBST) for every washing step: 3 quick washes followed by 3 washes for 20 min. The tubes covered with aluminum foil were placed on the nutator at room temperature (RT). A solution of 5 % normal goat serum (NGS) in PBST (NGS-PBST) was used for the preincubation of the brains for 1 h on the nutator at RT. Primary antibodies (mouse monoclonal anti-*Drosophila* ChAT antibody 4B1, DSHB; mouse anti-GFP antibody, A11120, Invitrogen; rabbit anti-GFP antibody, A11122, Invitrogen; rabbit GABA antibody, A2052, Sigma) of varying combinations were incubated at a concentration of 1:500 in NGS-PBST for 2 days on the nutator at 4°C. The brains were washed again in PBST 3 times quick and 3 x 20 min on the nutator at RT. The corresponding Secondary antibodies (Alexa Fluor® 488, goat anti-mouse IgG (H+L); Alexa Fluor® 488, goat anti-rabbit IgG (H+L); Alexa Fluor® 546, goat anti-rabbit IgG (H+L); Alexa Fluor® 633, goat anti-mouse IgG (H+L), all Invitrogen, Eugene, OR) were added at 1:500 to PBST and the incubation lasted for 2 days on the nutator at 4°C. Again the brains were washed in PBST 3 times quick and 3 x 20 min on the nutator at RT. The washing solution was replaced by Vectashield (Vector Laboratories, Inc., Burlingame, CA) for mounting. The brains within the mounting medium were transferred onto a microscope slide with a pipette tip, whose end was cut off. To prevent the brains

from floating away a bridge of sliced No. 2 coverslips (VWR, Darmstadt, Germany) was sealed with nail-polish to the microscope slide. With the anterior side facing upwards the brains adhered to the microscope slide and afterwards were covered with cover slips. The interspace was filled with mounting medium and the cover slip was also sealed with nail polish.

The brains were scanned with a Zeiss LSM 710 META confocal microscope (Carl Zeiss, Jena, Germany) set on a Smart Table UT2 (Newport Corporation, Irvine, CA) using a 40x water immersions objective (W Plan-Apochromat 40x/1.0 DIC M27; Carl Zeiss, Jena, Germany; Fig. 5). For the z-projections 1 µm intervals and a 1024 x 1024 pixel resolution were chosen. Zen 2009 Light Edition (Carl Zeiss MicroImaging GmbH, Germany) was used to generate images of the z-projections.

The number of the co-labeled projection neurons was counted in Amira 5.3 software (Visage Imaging, Berlin, Germany) using the Landmarks Editor.

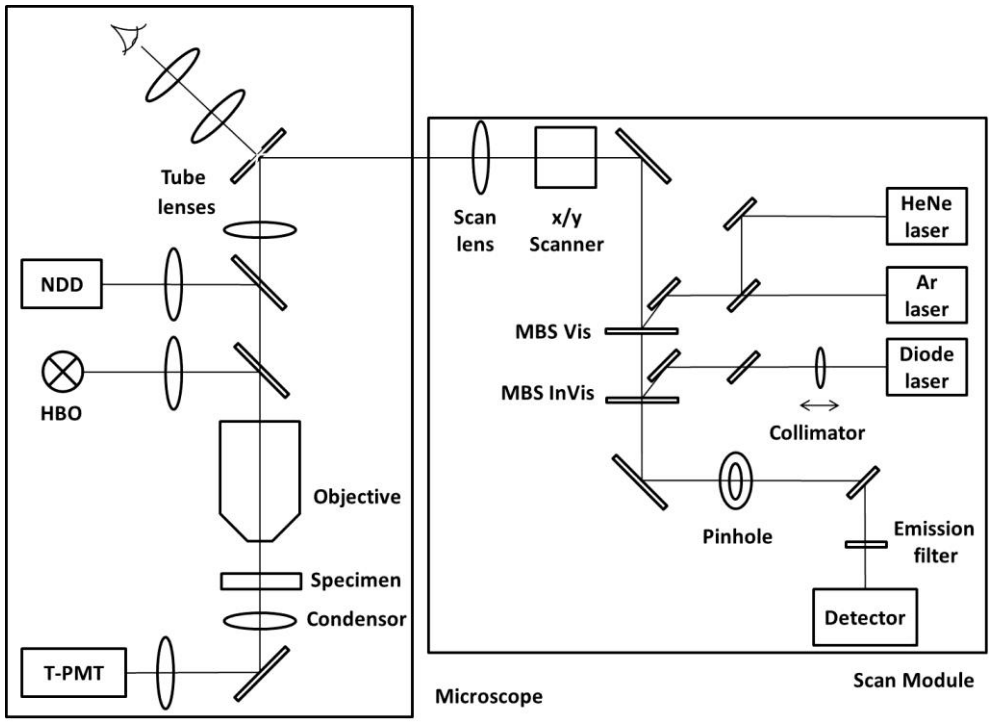

Fig. 5: Scheme of microscope setup. The specimen (either objective slice or purpose-made holder) is fixed on the piezostage, which is setting the position of the z-axis. The emissions by HeNe and Ar laser are detected with the detector in the scan module, emission by the diode laser is detected with the NDD. HBO Mercury Vapor Short-Arc Lamp; MBS Main Beam Splitter; NDD Non-Descanned Detector; T-PMT Transmission-Photomultiplier. (Adapted from Zeiss Operating Manual LSM 710, 2010.)

2.3 Preparation

For *in vivo* photoactivation experiments flies were dissected following the protocol described by Wilson *et al.* (2004) with a few modifications. Flies were separated in a vial and anesthetized for at least 15 min on ice. Grabbing the motionless flies on their legs enabled fixation in a custom-made stage (Fig. 6 B), which was a one-sided beveled plastic block of about 1 cm^3. On the upper edge of the beveled side was a drill-hole to give the fly its body enough free space when fixed. The notch deriving from the drill was covered with half of a 3.05 µm thin copper grid (Athene Grids ©) normally used for TEM microscopy. The neck of the fly was gently pushed into the slit of a 125 µm in the grid. To prevent the fly from moving, the head was fixed to the copper grid with Kolophonium (Royal oak, Rosinio, Germany) solubilized in 99 % ethanol. The salivary duct was cut shortly behind the salivary pump with a stab knife (Sharpoint, Surgical Specialties Corporation, Reading, PA) on the underside of the proboscis (Fig. 6 A) to prevent pumping and thereby moving of the brain. The tiny cut was occluded by the flexible membrane of the proboscis. To reduce the movement of the proboscis a minute needle (Austerlitz Insect Pins ®, Ø 0.1 mm) was laid across it and fixed on the left and right of the drill-hole with melted dental wax (Deiberit, Dr. Böhme & Schöps Dental GmbH) using a soldering-iron. When the Kolophonium mixture was dried after about 10 to 15 min, a fine wire (H.P. Reid Co. Inc., Palm Coast, FL) fixed with wax to a custom-made plastic coverslip (via Plano GmbH, order number L4193) was placed in the flexible ptilinal suture. The plate was fixed with wax to the beveled side of the plastic block. Turning screws, which passed through the block, bended the plate to tension the wire and resulting in a stretching of the antennae. A plastic plate with a window just a bit bigger than the entire fly head was placed on the head and fixed with wax to the top of the block. The margin of the window was placed next to the wire to cover the antennae and to leave the head capsule accessible for the dissection. With two-component silicone (Kwik-Sil™, WPI Inc, Sarasota, FL) the gap between head and margin of the plastic plate was sealed. Ringer solution (NaCl 7.6 g/l, KCl 0.37 g/l, $MgCl_2$ $6H_2O$ 0.41 g/l; $CaCl_2$ 2 H_2O 0.29 g/l; saccharose 12.32 g/l; HEPES 1.19 g/l; pH 7.3) was filled into the window of the plastic coverslip to prevent the fly from drying out while dissecting. With the stab knife a window was cut in the head capsule between the eyes and between the ocelli on the dorsal side as well as the ptilinal suture on the frontal side. Tracheae and fat bodies had to be removed to get a clear view onto the antennal lobes (Fig. 6 C).

The block with the dissected fly was placed under the objective of the two-photon laser scanning microscope (2P-LSM) using a Piezo-stage (PILine®, Physik Instrumente (PI) GmbH & Co. KG, Karlsruhe, Germany). The microscope is a Zeiss LSM 710 META confocal microscope

(Carl Zeiss, Jena, Germany) equipped with an infrared Chameleon Ultra ™ Diode-pumped Laser (Coherent, Santa Clara, CA) set on a Smart UT2 Table (Newport Corporation, Irvine, CA) (Fig. 5).

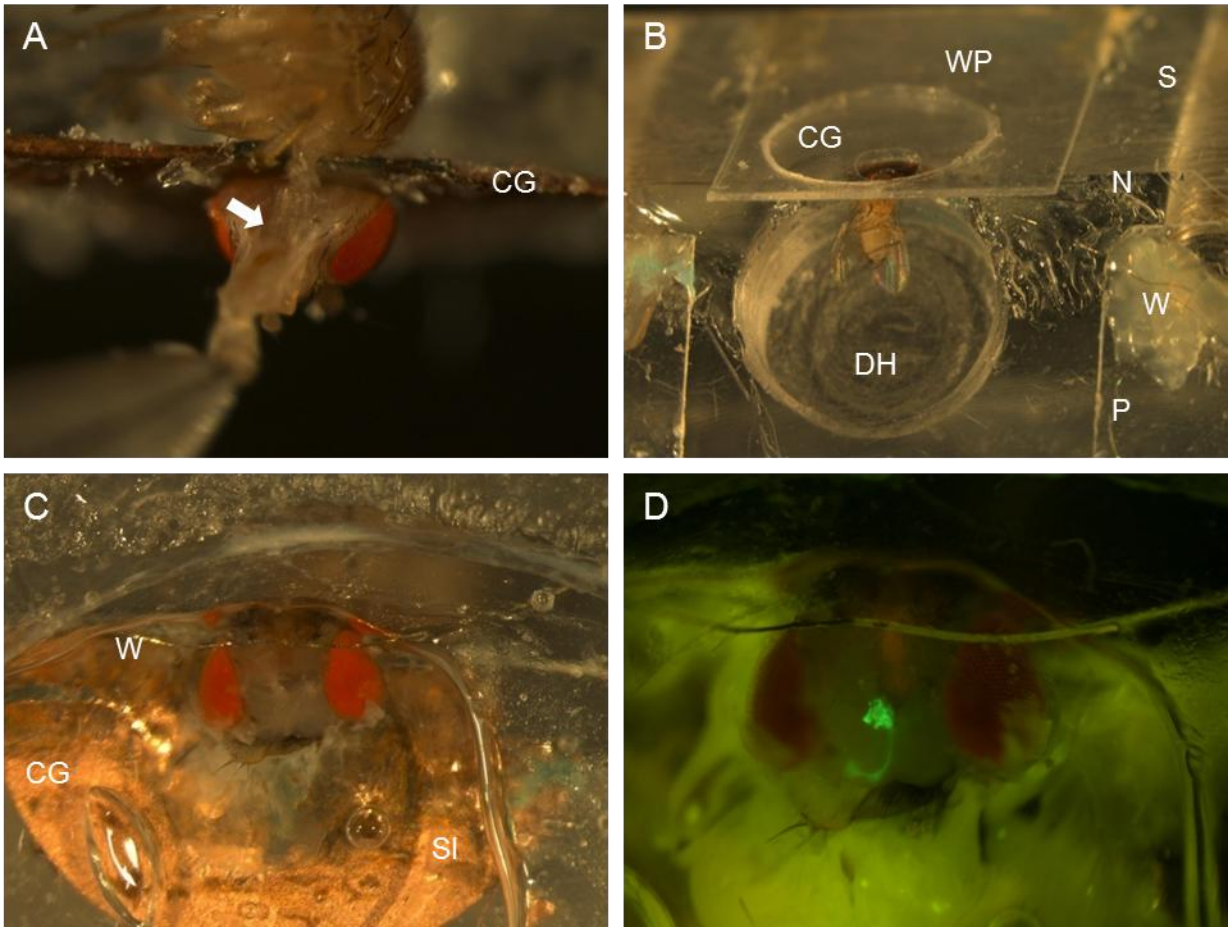

Fig. 6: Preparation of the fly and fixation in a custom-made stage. (A) Cut of the salivary duct (arrow) on the underside of the proboscis. (B) Fly fixed in one-beveled plastic block. (C) Removing of the head capsule to expose the brain. (D) After photoactivation of one antennal lobe a strong increase of the PA-GFP fluorescence is clearly visible. Abbreviations: CG copper grid; DH drill hole; N minute needle, P plastic plate; S screw; SI silicone; W wire; WP window plate.

2.4 Three-dimensional map

Due to the fact that projection neurons labeled by MZ699-GAL4 are multiglomerular and do not show strong glomerular innervation patterns as seen in the GH146-enhancer trap line, an additional staining of the glomerular structure was needed to allow a reliable detection and identification of single glomeruli. Therefore, *in vivo*-scans of OrX-GAL4-lines with the UAS-GC3.0-element recombined to END1-2 (see following table 1) were used to create a three-dimensional glomerular map of the antennal lobe of *in vivo* fly brains. These OrX-GAL4-lines show the innervation pattern of a single type of OSNs in their corresponding glomerulus (Fig. 7). On the basis of these innervations, glomeruli could be reliably identified in a z-scan combined with the END1-2-staining of the whole antennal lobe neuropil.

Table 1: OrX-GAL4-lines used for generating a 3D-map of glomeruli *in vivo*. The different glomeruli show distinct response pattern by odor-stimulation.

Genotype	Glomerulus	Best odor ligand
Or69a; END1-2,GC3.0; TM2/TM6B	D	
Or67d; END1-2,GC3.0; TM2/TM6B	DA1,VA6	*cis*-vaccenyl acetate
+; END1-2,GC3.0/+; Or56a/TM6B	DA2	
+; END1-2,GC3.0; Or42b	DM1	ethyl acetate
+; END1-2,GC3.0/Or22a; TM2/TM6B	DM2	ethyl hexanoate
Or47a; END1-2,GC3.0; TM2/TM6B	DM3	pentyl acetate
Or59b; END1-2,GC3.0; TM2/TM6B	DM4	methyl acetate
+; END1-2, GC3.0/Or67a; +/TM6B	DM6	ethyl benzoate
+; END1-2,GC3.0; IR75a	DP1l	
+; END1-2,GC3.0; Or92a	VA2	2,3-butanedione
+; END1-2,GC3.0; Or35a	VC3	1-hexanol
+; END1-2,GC3.0; Or43b	VM2, DM5	ethyl butyrate, ethyl 3-hydroxybutyrate
+; END1-2,GC3.0; Or42a	VM7	propyl acetate

The brains were scanned in multi-track mode (excitation wavelength used for GC3.0: 488 nm, for END1-2: 543 nm) at a Zeiss LSM 710 META confocal microscope (Carl Zeiss, Jena, Germany) set on a Smart UT2 Table (Newport Corporation, Irvine, CA) using a 40x water immer-

sions objective (W Plan-Apochromat 40x/1.0 DIC M27; Carl Zeiss, Jena, Germany; Fig. 5). For the z-projections 1 µm intervals and a 1024 x 1024 pixel resolution were chosen.

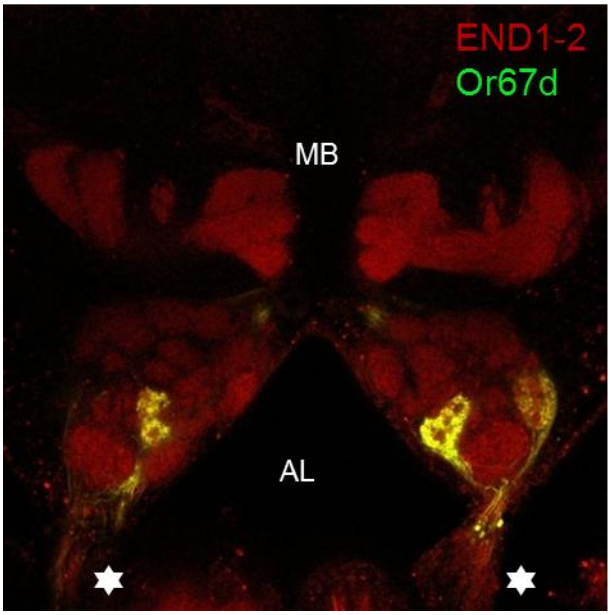

Fig. 7: Innervation pattern of the Or67d-GAL4 line labeling glomeruli DA1 and VA6 (green). END1-2-staining of the neuropil (red) allows the detection of the glomerular shape. AL antennal lobe; MB mushroom bodies; asterisks antennal nerve.

In order to get scans of the antennal lobe with an END1-2 staining showing a distinct glomerular shape, several flies were scanned. Finally, an *in vivo*-scan of the ALs of a fly with the genotype +; END1-2,C3PA; MZ699 was used for the labeling of single glomeruli in Amira 5.3 software (Visage Imaging, Berlin, Germany) using the Labelfield Editor. Comparison with scans of the varying OrX-GAL4 lines enabled the precise identification of the 15 corresponding glomeruli (table 1). Some prominent glomeruli were identified by comparison with the *in vitro* 3D-map of Couto *et al.* (2005). Especially the position of the glomeruli DA1 and VM2 and their neighboring glomeruli were important for the glomerular identification in the following photoactivation protocol.

2.5 Photoactivation

For photoactivation experiments in living flies the use of two-photon laser scanning microscopy (2P-LSM) was necessary to prevent the tissue from damage. 2P-LSM described by Denk *et al.* (1990) uses the molecular effect of simultaneously absorption of two photons with longer wavelength and lower energy (e.g. infrared light, IR) instead of absorbing one photon with shorter wavelength and higher energy (e.g. ultraviolet light, UV). For the absorption of two photons a required high density and flux of photons is offered by a pulsed laser. The energy of the two photons is in summation the same as the energy of the single photon, which is required to excite a fluorophore as e.g. PA-GFP. The excited fluorophore is emitting after a few nanoseconds a photon of longer wavelength as well as lower energy and the fluorophore drops down in the ground state. Excitation with lower energy reduces photobleaching of the fluorophores and photodamage to the tissue. In addition the 2P-LSM was used because of the sectioning effect so only a 2 µm slide around the focal plane is excited. This enables higher three-dimensional resolution and a higher precision for the photoactivation.

The protocol for the photoactivation was developed following the description by Datta *et al.* (2008). First I used the GH146-enhancer trap line (+; GH146; C3PA; A. Strutz) to test the functionality of the system and the expression of PA-GFP in olfactory projection neurons. Moreover I used these flies to check different scanning and excitation parameters in order to establish a protocol for the actual experiments using MZ699-GAL4. I started the test series using an excitation wavelength of 710 nm and different values for laser transmission (ranging from 7 to 16 percent) as well as different time series parameters (10 to 100 cycles, 10 to 40 s intervals). Unfortunately, this protocol resulted in strong photodamage in the majority of cases (Fig. 8).
To reduce the photodamage, the laser power was measured with a photometer (Coherent, Santa Clara, CA) under the objective, where the sample was normally placed. The laser power ranged from 1.5 mW to 15.5 mW at low scan speed. In comparison to the laser power of 5 up to 40 mW used by Datta *et al.* (2008) these values were surprisingly low and thus did not need to be further reduced. As a next step I varied the scanning mode using either the “time series” option or the “continuous mode”. Interestingly, the “time series” mode showed photodamage in the majority of cases, whereas the “continuous mode” revealed convincing results. Switching to the lower-energy wavelength 760 nm (with transmission of laser power compared to 710 nm) revealed a shorter activation time and a decrease in photodamage of the tissue. Finally, I used the following parameters for the photoactivation: a) excitation wavelength: 760 nm, b) transmission: 3 or 4 % (this is equivalent to ~ 1.3 mW), c) 1.58 or 6.3 µs pixel dwell and d) a pixel average of

4. Z-stacks before and after photoactivation for comparison were scanned with a wavelength of 925 nm, which is not influencing the photoactivation. The region for the illumination was defined in the z-stack for flies of the genotype +; GH146; C3PA and for +; END1-2,C3PA; MZ699 flies by using the He/Ne-laser with 543 nm-wavelength - the excitation wavelength of DsRed - which enables identification of distinct glomeruli. The flies were scanned with a Zeiss LSM 710 META confocal microscope (Carl Zeiss, Jena, Germany) equipped with an infrared Chameleon Ultra ™ Diode-pumped Laser (Coherent, Santa Clara, CA) set on a Smart UT2 Table (Newport Corporation, Irvine, CA) using a 40x water immersions objective (W Plan-Apochromat 40x/1.0 DIC M27; Carl Zeiss, Jena, Germany; Fig. 5). For the z-projections 1 µm or 3 µm intervals and a 1024 x 1024 pixel resolution were chosen.

The software Zen 2009 Light Edition (Carl Zeiss MicroImaging GmbH, Germany) was used to generate images of the z-projections.

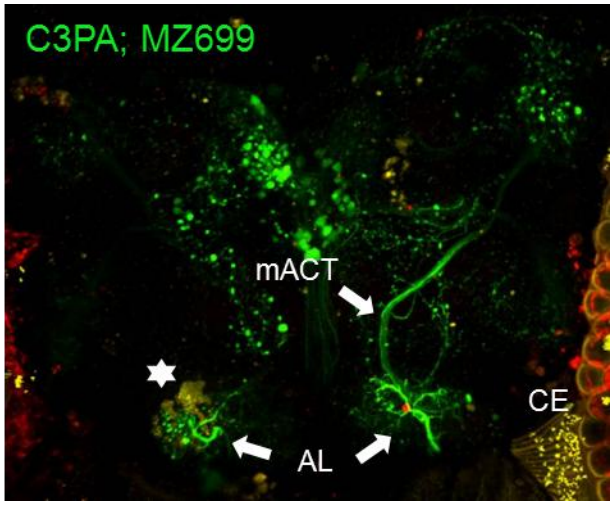

Fig. 8: Photodamage (marked by the asterisk) caused by irradiation with 710 nm-wavelength while scanning in time series-mode. AL antennal lobe; CE compound eye; mACT medial antenno-cerebral tract.

3. Results

The olfactory PNs labeled by the enhancer trap line MZ699-GAL4 were analyzed in detail using immuno-histological techniques as well as genetic tools to characterize their neuronal properties and anatomy. These data will help drawing conclusions regarding their putative role for odor coding and processing in the *Drosophila* olfactory system.

3.1 Immunostaining against GABA and ChAT

The type of expressed neurotransmitter in MZ699-PNs was analyzed by immunostaining against the inhibitory neurotransmitter GABA, and against the enzyme ChAT, that is producing the excitatory neurotransmitter ACh.

Anti-GABA immunostaining showed a widespread labeling of structures in the whole brain. An extensive labeling of the synaptic terminals of different neurons innervating the AL enabled to define the borders of single glomeruli. Labeled cell clusters lay around the AL (Fig. 9 A1) and the SOG; lateral to the LH, as well as between the deuterocerebrum and the lobula. Interestingly, GABA was also detected in the neurites. These GABAergic neurites extended from the cell cluster dorsal to the AL to the ellipsoid body and the fan shaped body as well as the MB calyx and the LH. Interestingly in some brains the stained dorsal giant interneuron (DGI) and a weak GABA-labeling of the MB-γ lobe were discernible (data not shown). Dual-staining with anti-GABA and anti-GFP revealed GABA expression in several somata of PNs labeled by the MZ699-GAL4 line (Fig. 9 A). Interestingly, somata lying most anterior in the ventral cell cluster were not GABAergic, but the GABAergic somata were grouped next to the AL. Some neurites of MZ699-PNs were stained by anti-GABA immunostaining as well. That was discernible in projections leaving the AL and extending to the LH (Fig. 9 D). But not all arborizations in the LH showed labeling by GABA-immunostaining. This confirms the assumption that some PNs in MZ699 are expressing the inhibitory neurotransmitter GABA (Okada *et al.*, 2009).

Analysis of the first scanned immunostainings revealed a variability in the number of MZ699-PNs expressing GABA, potentially dependent on the age of the fly. To verify this, the number of PNs and of GABA-expressing PNs was enumerated (see table in appendix for detailed numbers). It was sometimes difficult to differentiate between the somata of PNs and somata of the SOG-neurons, whose cell clusters lay close to each other, but in most cases the corresponding

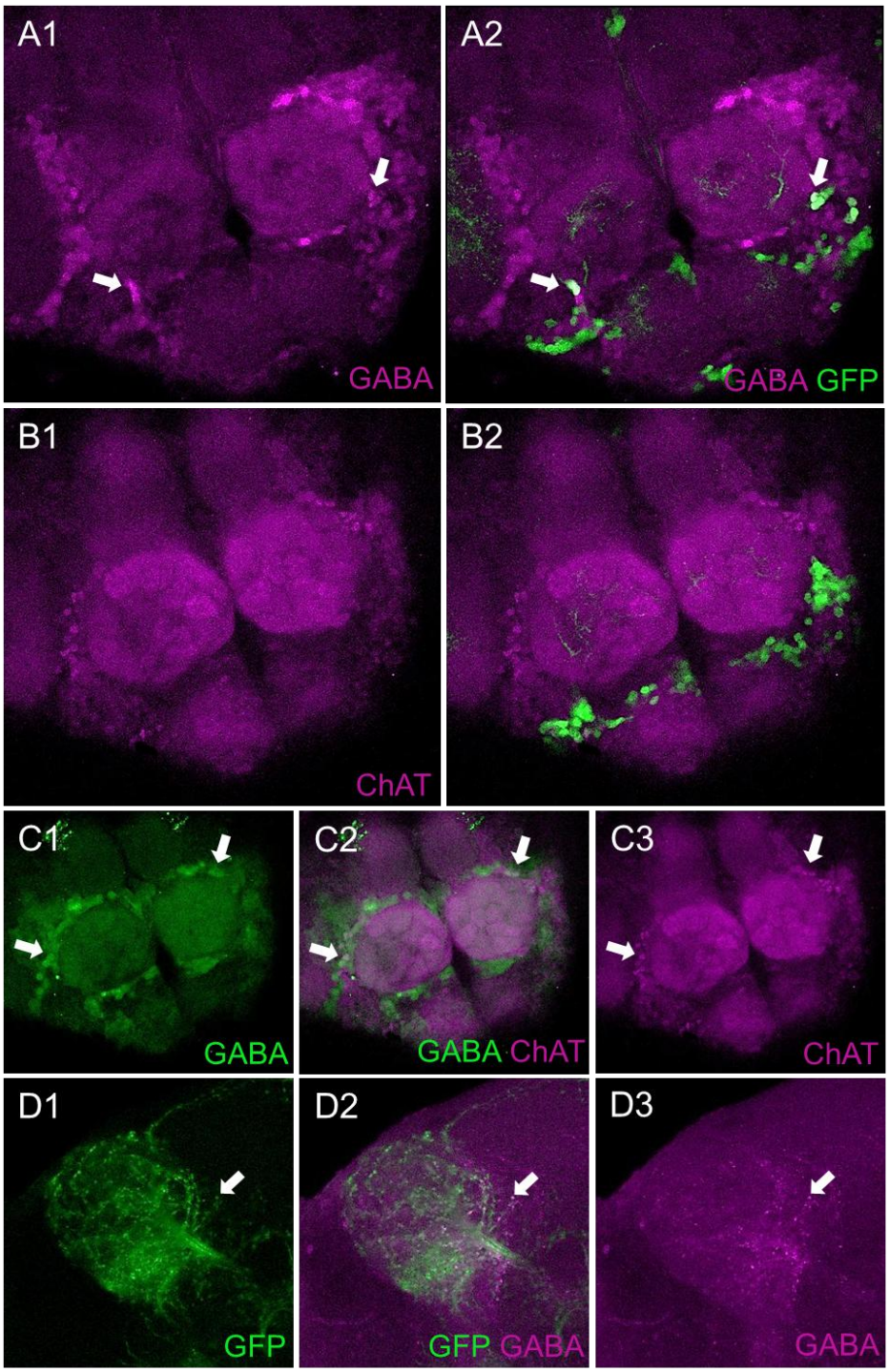

Fig. 9: Expression of different neurotransmitter in MZ699-PNs. (A1) Cell clusters around the AL and glomeruli are labeled in anti-GABA immunostaining. (A2) GABA-expression (magenta) in MZ699-PNs (green) appears white in the merged image (arrows). (B1) Cell cluster dorso-lateral to the AL and glomeruli are labeled in anti-ChAT immunostaining. (B2) Immunostaining revealed no expression of ChAT (magenta) in MZ699-PNs (green). Expression of GABA (green; C1) and ChAT (magenta; C3) in single LNs (C2; arrows). The merged image (D2) shows expression of GABA (magenta; D3) in MZ699-PNs (green; D1) projecting into the LH. Dorsal is up.

neurites indicated their affiliation. Also, the intensity of GABA and GFP-staining increased in an age-dependent way, possibly due to an accumulation of these molecules with increasing age.

Table 2 and figure 10 show that the number of PNs and GABAergic PNs rised depending on the age of the fly. Five hours after hatching the flies had a median of 38 PNs and about six of them were GABAergic. Old flies with an age of 13 to 15 days had a median of 50 PNs with about 17 of them expressing GABA. This was an increase of more than the double number of the GABAergic PNs. But as shown in table 2 there was a high variability in the number of cells at every age analyzed. The reason for this variability is so far unknown and has to be analyzed in further experiments.

Table 2: Variability in the number of MZ699-PNs expressing GABA depending on the age of flies. Lowest and highest numbers of counted cells in individual flies of different age, the median of these numbers and the corresponding standard deviations (SD) are given in the table.

Age	Number of PNs	Median number of PNs ± SD	Number of GABAergic PNs	Median number of GABAergic PNs ± SD	Percentage of GABAergic PNs
5 h	32 - 43	38 ± 2.9	5 - 12	6 ± 2.3	15.8
2-3 d	35 - 48	42 ± 4.2	3 - 17	8 ± 3.5	19.0
4-6 d	35 - 61	44.5 ± 7.5	4 - 47	10 ± 11.4	22.5
7-9 d	37 - 64	46 ± 6.5	8 - 25	11 ± 4.1	23.9
11-12 d	40 - 55	48 ± 3.9	12 - 18	15 ± 3.0	31.3
13-15 d	42 - 55	50 ± 4.7	6 - 19	17 ± 5.1	34

Immunostaining with anti-ChAT also showed a widespread labeling of structures in the whole brain. Single glomeruli were discernible because of the extensive labeling of the synaptic terminals of different neurons innervating the AL. Similarly to the GABA-immunostaining, labeled cell clusters lay around the AL (Fig. 9 B1) and the SOG; lateral to the LH, as well as between the deuterocerebrum and the lobula. In comparison to cells labeled by anti-GABA the cell bodies labeled by ChAT-antibodies were smaller and no labeled neurites were discernible. Dual-staining with anti-ChAT and anti-GFP showed no expression of ChAT in somata of MZ699-PNs (Fig. 9 B). Hence, MZ699-PNs do not contain the excitatory neurotransmitter ACh.

Interestingly, I found a few anti-GABA and anti-ChAT co-labeled cell bodies on the dorsal side of the AL (Fig. 9 C). These cells were not MZ699-PNs, whose somata lay in the ventral cell cluster. Possibly, these were LNs, but this needs to be analyzed in further experiments.

Comparing anti-GFP-immunostainings of flies with the genotypes +; GC3.0; MZ699 (A. Strutz) and +; UAS-GFPnls; MZ699 (Y. Seki) showed no differences in the GFP-expression pattern of neurons labeled by the MZ699-GAL4 line. Although the line UAS-GFPnls should result in a GFP expression only in the nucleus, the whole neurites were labeled. Occasionally, several neurons were labeled additionally in the MZ699-GAL4 line, which are not described by Ito *et al.* (1997). These were Kenyon cells (KC) and fibers in α- and β-lobes of the MBs inclusively the calyx, as well as cells innervating the lobula. Expression in these neurons could derive from the transient activation of the corresponding promoter (personal communication from A. Strutz and R. Benton). Investigations of the circumstances evoking this additional activation of the promoter have not been examined further and thus would be beyond the scope of this thesis.

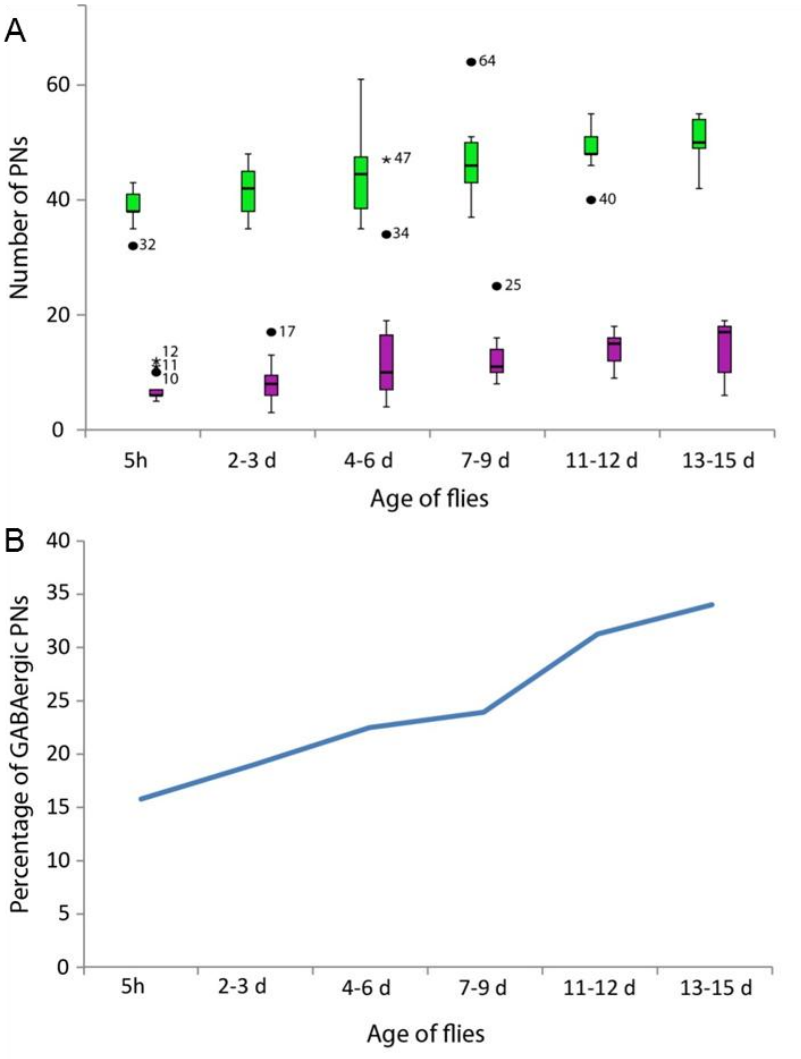

Fig. 10: (A) Boxplots representing the number of GABAergic PNs (magenta) in comparison to the total number of MZ699-PNs (green) depending on the age of flies. (B) The percentage of GABAergic PNs (blue line) shows the age-dependent increase.

3.2 Three-dimensional map of *in vivo* fly antennal lobes

The enhancer trap line MZ699 shows a weak multiglomerular innervation pattern. To analyze the innervation pattern of single glomeruli in flies using photoactivation a 3D-map of all glomeruli in the AL was necessary. In a fly of the genotype +; END1-2,C3PA; MZ699 stained glomeruli were labeled and as far as possible identified.

The generation of this 3D-map (Fig. 11) by comparing shape and position of the glomeruli in the scans of the varying OrX-GAL4 lines revealed differences in shape and position of some glomeruli as well as in the shape of the whole AL compared to the reconstructions of *in vitro*-scans I generated for Seki *et al.* (2010). These observed differences probably derive from the intact antennal nerve that tensions the AL. The AL showed a spindle shape *in vivo,* and a flattened spherical shape *in vitro* (Fig. 11 D). Likewise, all glomeruli showed a flattened shape *in vitro*. For example, the glomeruli VA5, DA3 and all DM-glomeruli were longish in the *in vivo*-brains, but they show a globular shape *in vitro*. The position of the glomerulus DL3 for example differed between scans that were done with *in vivo*-brains compared to *in vitro*-brains. *In vivo* DL3 was located in plane with the DA1 and DA3 glomeruli, furthermore between the glomeruli DA1, DL2d, DL1 and DL3 an interspace was discernible. In contrast the DL3-glomerulus seems to be shifted between the glomeruli DL2d and DL1 *in vitro*. Another difference is, that the glomeruli VM1, VM4, VM6 and V were not laying as an apart group on the ventral, posterior side of the AL as it is discernible in *in vitro*-scans. The VM2- and DA1-glomeruli, which I mainly used for the photoactivation experiments, showed no significant difference in shape and position between *in vivo* and *in vitro* fly brains. Glomerulus VM2 has a triangular shape and is positioned ventral, medial neighboring to the glomeruli VA2 and VM3. Therefore, this glomerulus can be identified easy. The DA1-glomerulus is positioned on the anterior lateral side of the AL next to the other prominent glomeruli VA1d and VA1v, and can also be identified easily.

The 3D-map is not yet completed, because not all glomeruli could be identified precisely. Beside the 15 glomeruli identified by the innervations of the OrX-GAL4 lines 16 other glomeruli (DA3, DC1 and DC3, DL2d and DL2v, DL3, DL4 and DL5, DP1m, VA1, VA3, VL1, VL2a and VL2p, VM3 and VM6) could be identified precisely by their shape and position compared to the *in vitro* reconstruction by Couto *et al.* (2005). Some glomeruli, as VC1, VC2, VM1, VM5d and VM5v, 1, as well as VA7m and VA7l could however not be labeled with certainty, because they show also a broad variety in shape in the *in vitro* 3D-reconstructions. These have to be labeled by using further OrX-GAL4 lines, which were not available for me during my thesis.

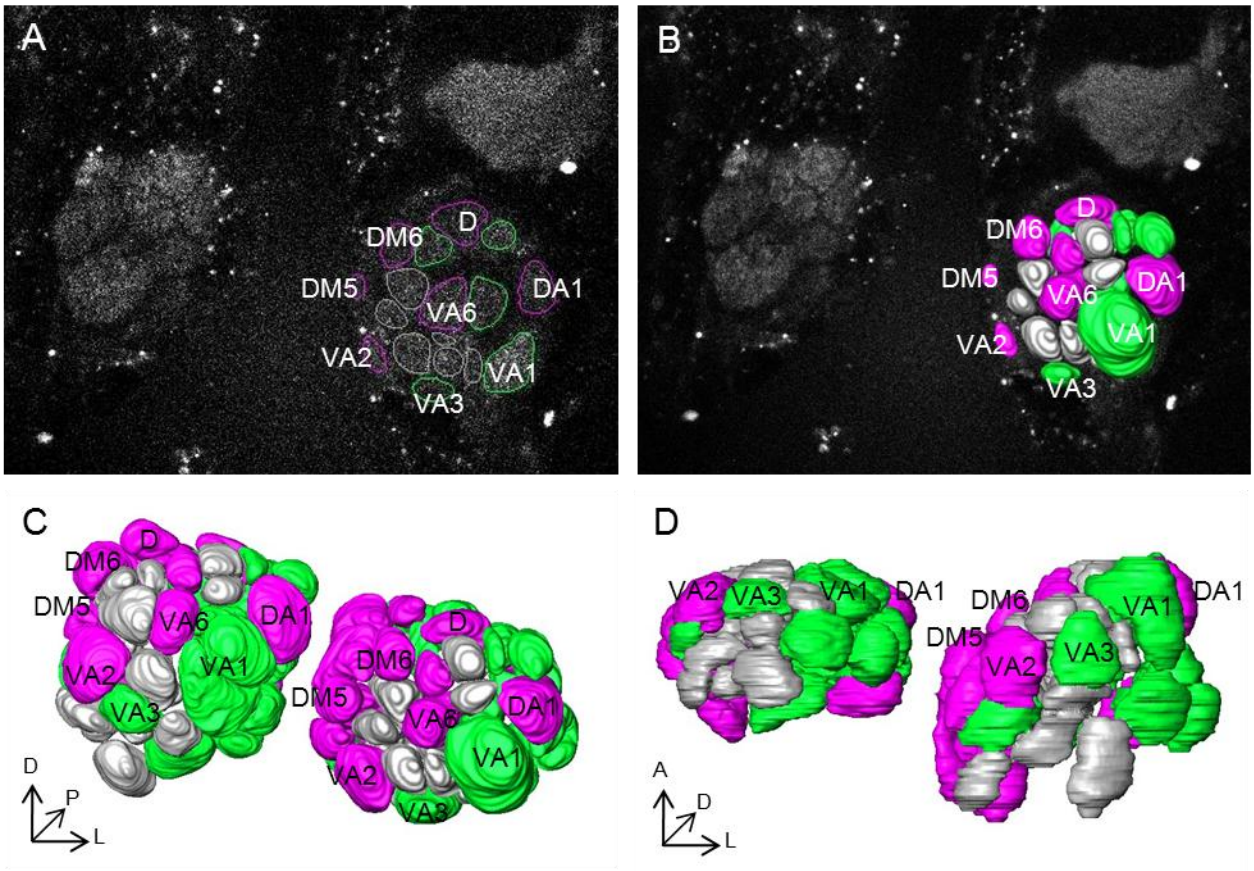

Fig. 11: 3D-reconstruction of the antennal lobe in Amira 5.3. Glomeruli in magenta are identified by OrX-GAL4 lines, glomeruli in green are identified by comparison to the 3D-map of Couto *et al.* (2005), glomeruli in gray can not be identified precisely. (A) Slice of the scan with labeled glomeruli in one AL. Only some glomeruli are named. Dorsal is up. (B) 3D-reconstruction of the labeled glomeruli. Dorsal is up. (C) Comparison of shape and position of glomeruli *in vitro* (left) and *in vivo* (right). (D) Comparison of the shape of the AL *in vitro* (left) and *in vivo* (right).

3.3 Photoactivation of GH146- and MZ699-GAL4 enhancer trap lines

The photoactivation experiments always started with scanning a z-stack with a wavelength of 925 nm to determine the pre-activation state of the GAL4 line under consideration. Due to the fact that the excitatory PNs that are labeled by the GH146-GAL4 line show exclusively uniglomerular innervation patterns in the AL, single glomeruli could easily be identified that were subsequently used to define a region for the photoactivation. The result of the photoactivation process was scanned afterwards again as a z-stack at the wavelength of 925 nm. The software Zen 2009 Light Edition (Carl Zeiss MicroImaging GmbH, Germany) was used to generate images of the z-projections. Values of brightness, contrast and gamma were varied to optimize the fluorescent properties of the samples.

To test the functionality of PA-GFP in flies carrying the genotype +; GH146-GAL4; UAS-C3PA the whole AL was exposed to light of 760-nm wavelength in a continuous light exposure mode. The photoactivated structures showed a strong increase of the fluorescence signal in compari-

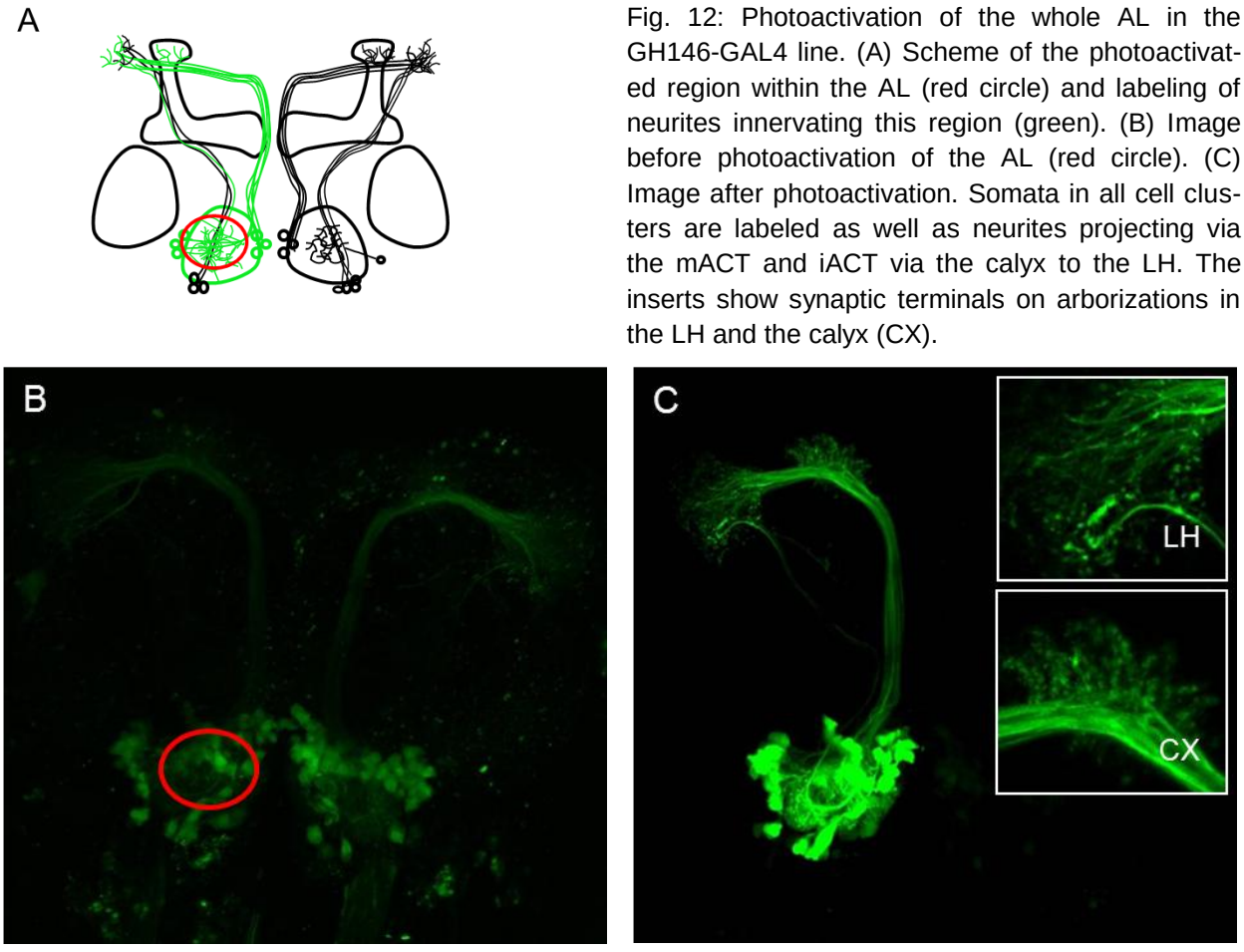

Fig. 12: Photoactivation of the whole AL in the GH146-GAL4 line. (A) Scheme of the photoactivated region within the AL (red circle) and labeling of neurites innervating this region (green). (B) Image before photoactivation of the AL (red circle). (C) Image after photoactivation. Somata in all cell clusters are labeled as well as neurites projecting via the mACT and iACT via the calyx to the LH. The inserts show synaptic terminals on arborizations in the LH and the calyx (CX).

son to the non-activated structures. A strong fluorescence signal was visible in the somata of the anterodorsal, lateral and ventral cell clusters after photoactivation of the whole AL (Fig. 12). The tracts appeared in a few samples dark on the level of the MB lobes. This could be due to the accumulation of only a low number of photoactivated molecules in small structures as e.g. axons with tiny diameters. Three or four neurites were projecting exclusively via the mACT into the LH but the majority projected via the iACT into the calyx and the LH. In the LH only very few bouton-like synaptic terminals were visible per arborizations (insert in Fig. 12 C). In contrast in the calyx region several synaptic terminals occurred next to each other and were densely packed on short arborizations (insert in Fig. 12 C). In comparison to the neurites the synaptic terminals showed a brighter fluorescence signal and had a nearly two times bigger diameter. Interestingly, a few labeled neurites projected from the LH to a region located posterior to the MB lobes (not shown).

To label all GH146-neurons, that are innervating the LH, I photoactivated a small region in the LH. Photoactivation of the LH showed a weaker fluorescence signal of glomeruli and somata

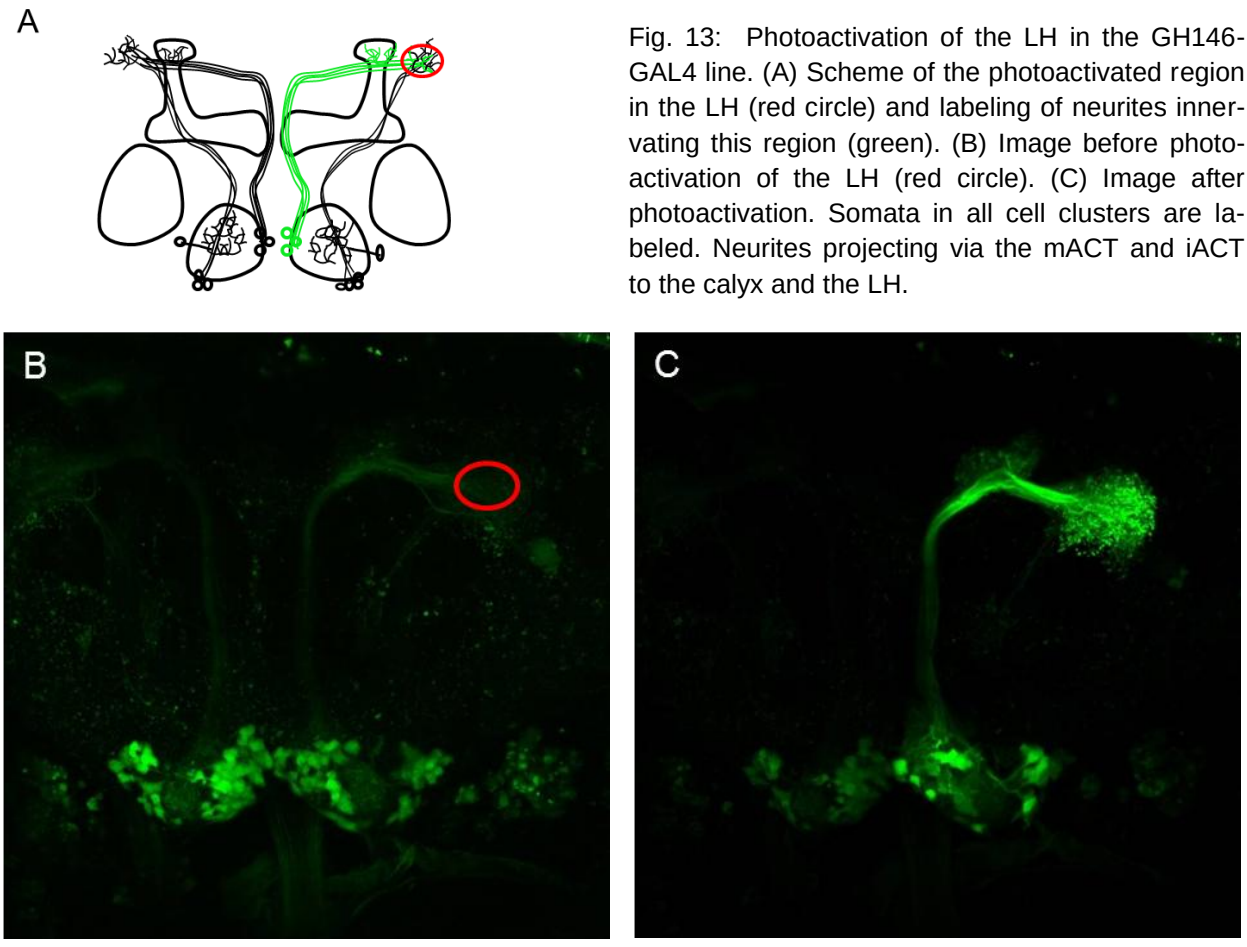

Fig. 13: Photoactivation of the LH in the GH146-GAL4 line. (A) Scheme of the photoactivated region in the LH (red circle) and labeling of neurites innervating this region (green). (B) Image before photoactivation of the LH (red circle). (C) Image after photoactivation. Somata in all cell clusters are labeled. Neurites projecting via the mACT and iACT to the calyx and the LH.

(Fig. 13) compared to the photoactivation of the whole AL. Neurites projecting via the mACT to the LH were labeled only rarely depending on the position of the photoactivated region in the LH. Since the mACT projected either directly to the LH or otherwise conjoined with the iACT shortly before reaching the LH, the position of photoactivation was crucial for hitting the mACT. In addition the low rate of labeling the mACT might be due to the low number of PNs following the mACT to the LH which comprises about three GH146-PNs. Interestingly, some neurites were labeled that projected from the LH to a region located posterior to the MB lobes (not shown).

In order to label only subsets of PNs that innervate a single glomerulus I photoactivated the DA1-glomerulus, that encodes the so far only known sex pheromone in *Drosophila*, which is 11-*cis*-vaccenyl acetate. The photoactivation of DA1 (Fig. 14) showed a strong innervation pattern within the DA1-glomerulus and a weak labeling of sparse arborizations in other glomeruli (white arrow in Fig. 14 C). Furthermore, 6 to 11 somata were labeled, that were all located in the lateral cell cluster, except one soma that was located in the ventral cluster. Before leaving the AL

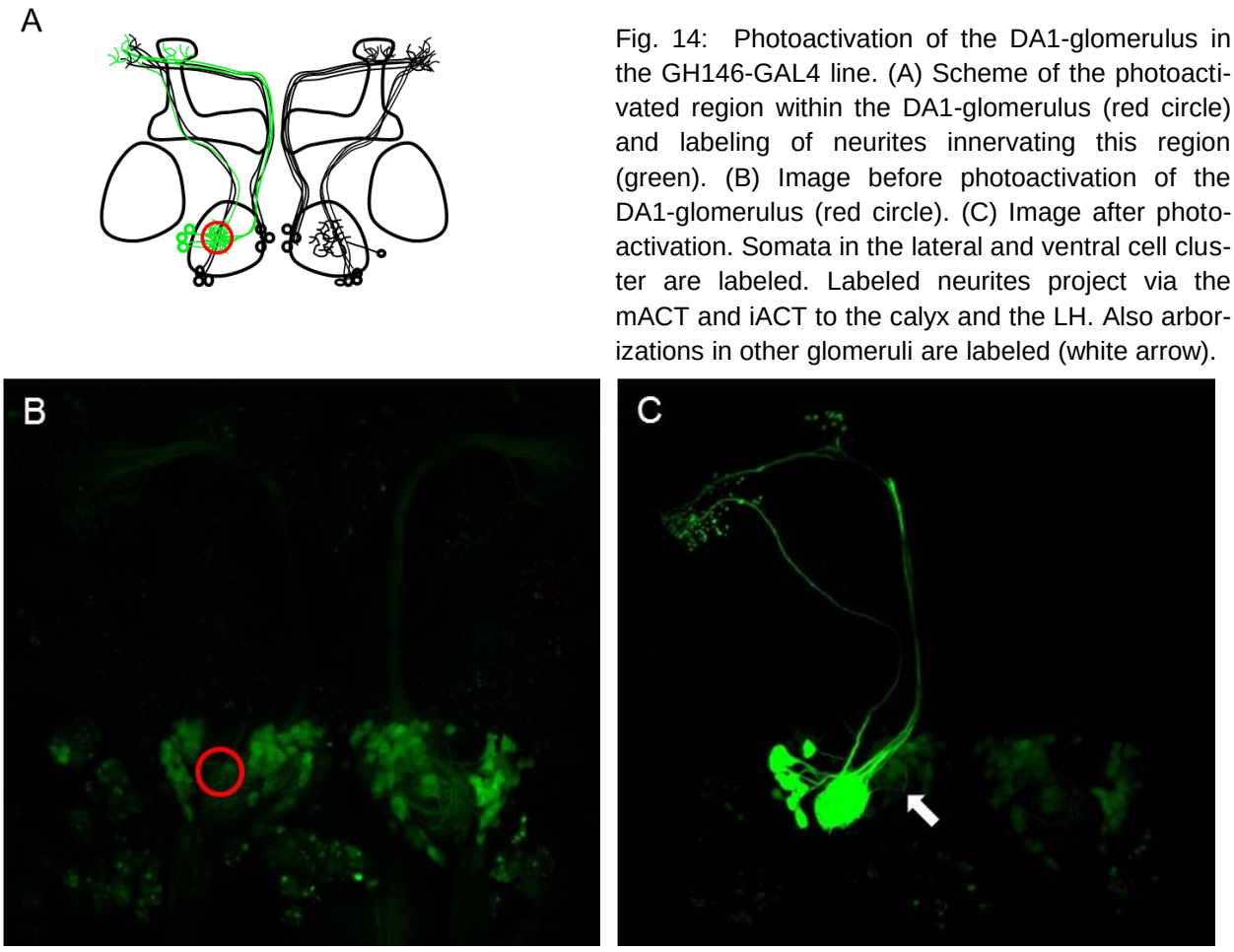

Fig. 14: Photoactivation of the DA1-glomerulus in the GH146-GAL4 line. (A) Scheme of the photoactivated region within the DA1-glomerulus (red circle) and labeling of neurites innervating this region (green). (B) Image before photoactivation of the DA1-glomerulus (red circle). (C) Image after photoactivation. Somata in the lateral and ventral cell cluster are labeled. Labeled neurites project via the mACT and iACT to the calyx and the LH. Also arborizations in other glomeruli are labeled (white arrow).

the neurites conjoined to three neurites innervating the LH. One of these labeled neurites projected via the mACT into the LH. The two other neurites innervated the calyx and the LH via the iACT. A few short arbors innervated the calyx and these arbors showed no further arborizations. Only the ventral part of the LH was innervated by the labeled neurites. The synaptic terminals of the neurites projecting into the LH via the mACT showed a stronger fluorescence signal than synaptic terminals of the neurites projecting via the iACT. This diverging intensity could result from a different number of photoactivated molecules per neuron and/ or a different distribution of activated molecules depending on diffusion. Future experiments should be dedicated to further analyze the innervation pattern of single neurons innervating the DA1-glomerulus to characterize their anatomy in detail.

In another set of experiments the glomerulus VM2 was photoactivated to visualize its innervating PNs. The glomerulus VM2 has been shown to code odors that are behaviorally attractive (Stökl *et al.*, 2010). After the photoactivation of glomerulus VM2 (Fig. 15) labeled neurites showed arborizations in other glomeruli on the ventrolateral side of the AL (white arrow in Fig.

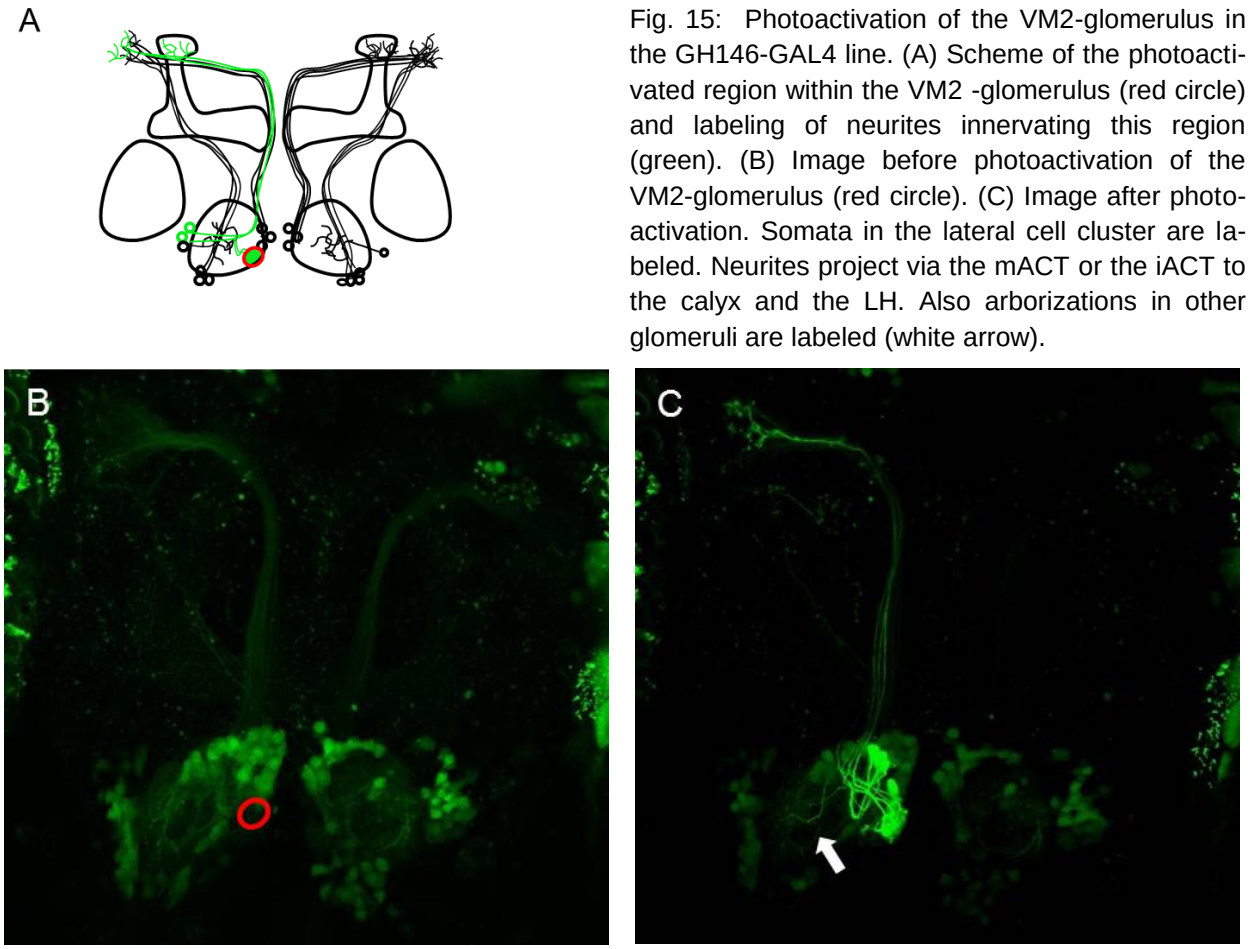

Fig. 15: Photoactivation of the VM2-glomerulus in the GH146-GAL4 line. (A) Scheme of the photoactivated region within the VM2 -glomerulus (red circle) and labeling of neurites innervating this region (green). (B) Image before photoactivation of the VM2-glomerulus (red circle). (C) Image after photoactivation. Somata in the lateral cell cluster are labeled. Neurites project via the mACT or the iACT to the calyx and the LH. Also arborizations in other glomeruli are labeled (white arrow).

15 C) and five somata were labeled. These adjoining somata were located in the anterodorsal cell cluster. Two of the labeled neurites innervated the ventral part of the LH via the mACT. In the LH it appeared that these neurites had synaptical connections to neurons innervating the MB. The three other neurites innervated the LH via the iACT. Within the LH they were located so close to each other by showing a similar innervation pattern, that it seemed, that the LH was innervated by one projection only. During the photoactivation experiments of the VM2-glomerulus the DM5-glomerulus was often labeled as well suggesting a connection between these two glomeruli. Two somata in the lateral cell cluster were then labeled in addition. Fig. 15 C shows a partial labeling of the DM5-glomerulus without the additional labeled soma. Thus it seems that some neurites innervate both glomeruli. In further analyses it has to be determined if some neurons innervate both glomeruli or if this labeling is an artifact due to the neighboring position and thus a consequential photoactivation.

Since the photoactivation of the two glomeruli DA1 and VM2 showed a characteristic labeling of

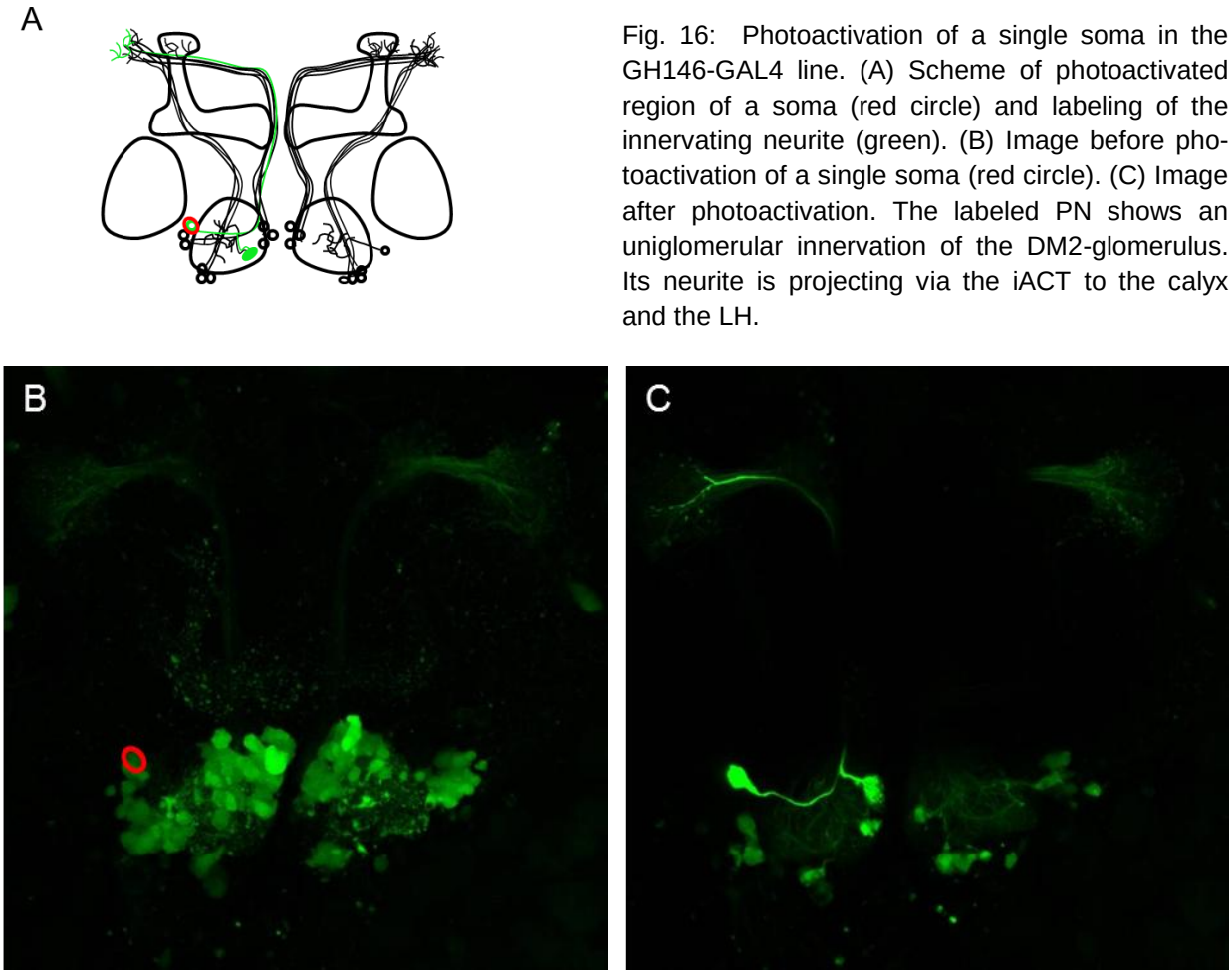

Fig. 16: Photoactivation of a single soma in the GH146-GAL4 line. (A) Scheme of photoactivated region of a soma (red circle) and labeling of the innervating neurite (green). (B) Image before photoactivation of a single soma (red circle). (C) Image after photoactivation. The labeled PN shows an uniglomerular innervation of the DM2-glomerulus. Its neurite is projecting via the iACT to the calyx and the LH.

the corresponding somata as well as the labeled neurites, I aimed to activate single somata in order to visualize single PNs. The main sources of error here were the direct vicinity and the overlap in the z-axis of single cell bodies as well as the slight movement artifacts of the brain. In several attempts unfortunately more than one cell body was labeled. However, the labeling of single somata was finally successful and is represented as an example in Fig. 16. The labeled PN innervated one single glomerulus, which could subsequently be identified as glomerulus DM2.

In summary a protocol of photoactivation was established successful for the labeling of GH146-PNs, which allows the identification of single PNs and their innervated target regions. The same protocol was subsequently used for photoactivation experiments of the enhancer trap line MZ699 in order to enable a morphological analysis of inhibitory PNs.

Due to the fact that PNs labeled by the MZ699-GAL4 line show multiglomerular and thus very sparse innervation patterns in the AL, the identification of single glomeruli was very difficult.

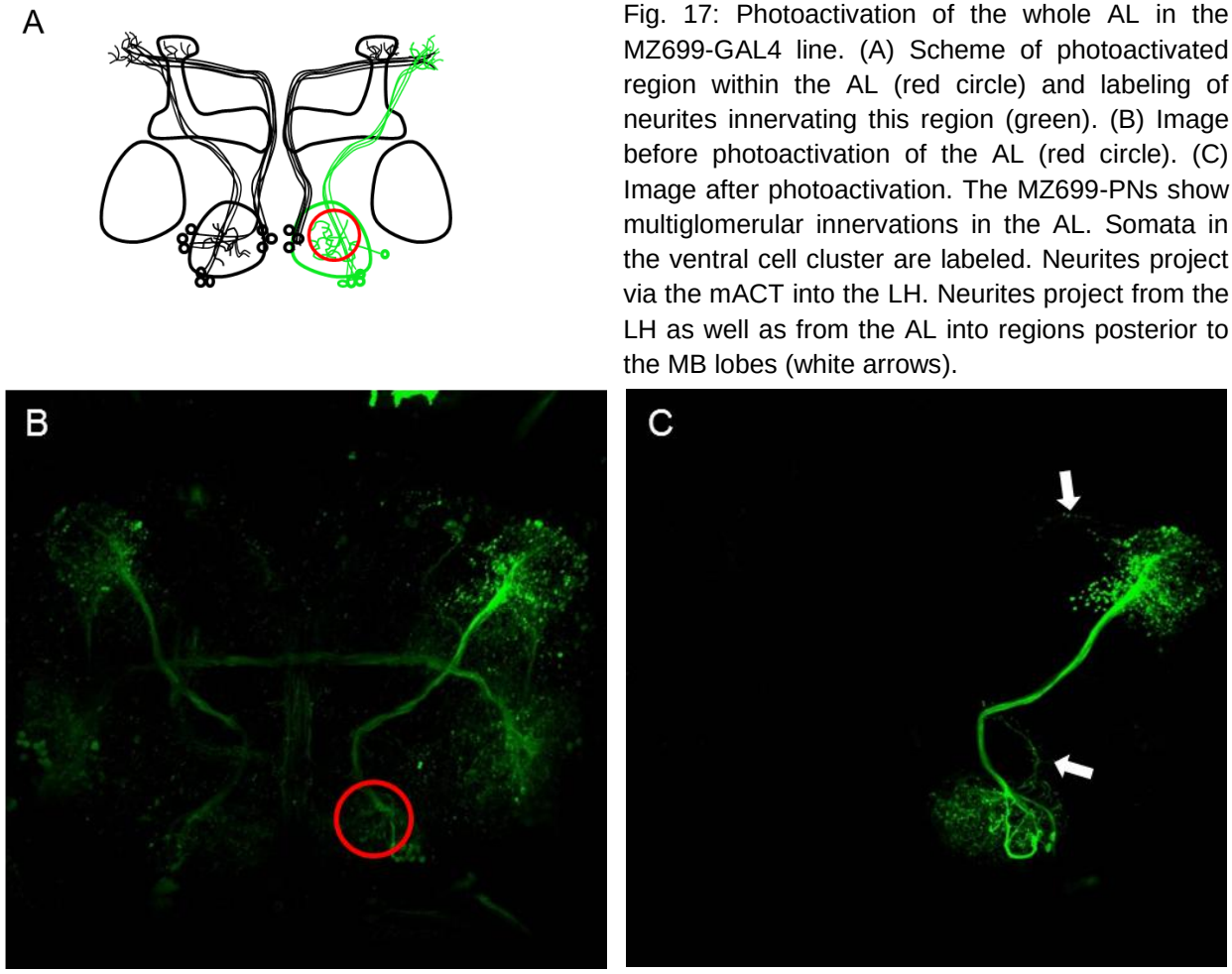

Fig. 17: Photoactivation of the whole AL in the MZ699-GAL4 line. (A) Scheme of photoactivated region within the AL (red circle) and labeling of neurites innervating this region (green). (B) Image before photoactivation of the AL (red circle). (C) Image after photoactivation. The MZ699-PNs show multiglomerular innervations in the AL. Somata in the ventral cell cluster are labeled. Neurites project via the mACT into the LH. Neurites project from the LH as well as from the AL into regions posterior to the MB lobes (white arrows).

Hence, I used flies that expressed the marker UAS-DsRed fused to synaptobrevin to label the whole neuropil in the living fly separately. Since the excitation wavelength of DsRed is 543 nm, additional scans for several focal planes were performed with this wavelength. After identification of the region of interest for the photoactivation in the DsRed labeling, the same protocol was used as applied for the experiments with the GH146-GAL4 line. The only difference was the time duration of photoactivation which was 15 min for the GH146-GAL4 line and 25 min for the MZ699-GAL4 line.

First of all, the pre-activation fluorescence signal of PA-GFP was much weaker in the MZ699-GAL4 line in comparison to the GH146-GAL4 line. In order to visualize all MZ699-neurons, that are receiving an olfactory input, I photoactivated the whole AL, that resulted in a stronger fluorescence signal in comparison to the non-photoactivated regions (Fig. 17). Interestingly, relatively small somata in the ventral cell cluster were labeled with only a weak fluorescence signal. An apparently random innervation of the glomeruli verified the multiglomerular innervation pattern of the MZ699-GAL4 line. Interestingly, two neurites projected from the AL into a region pos-

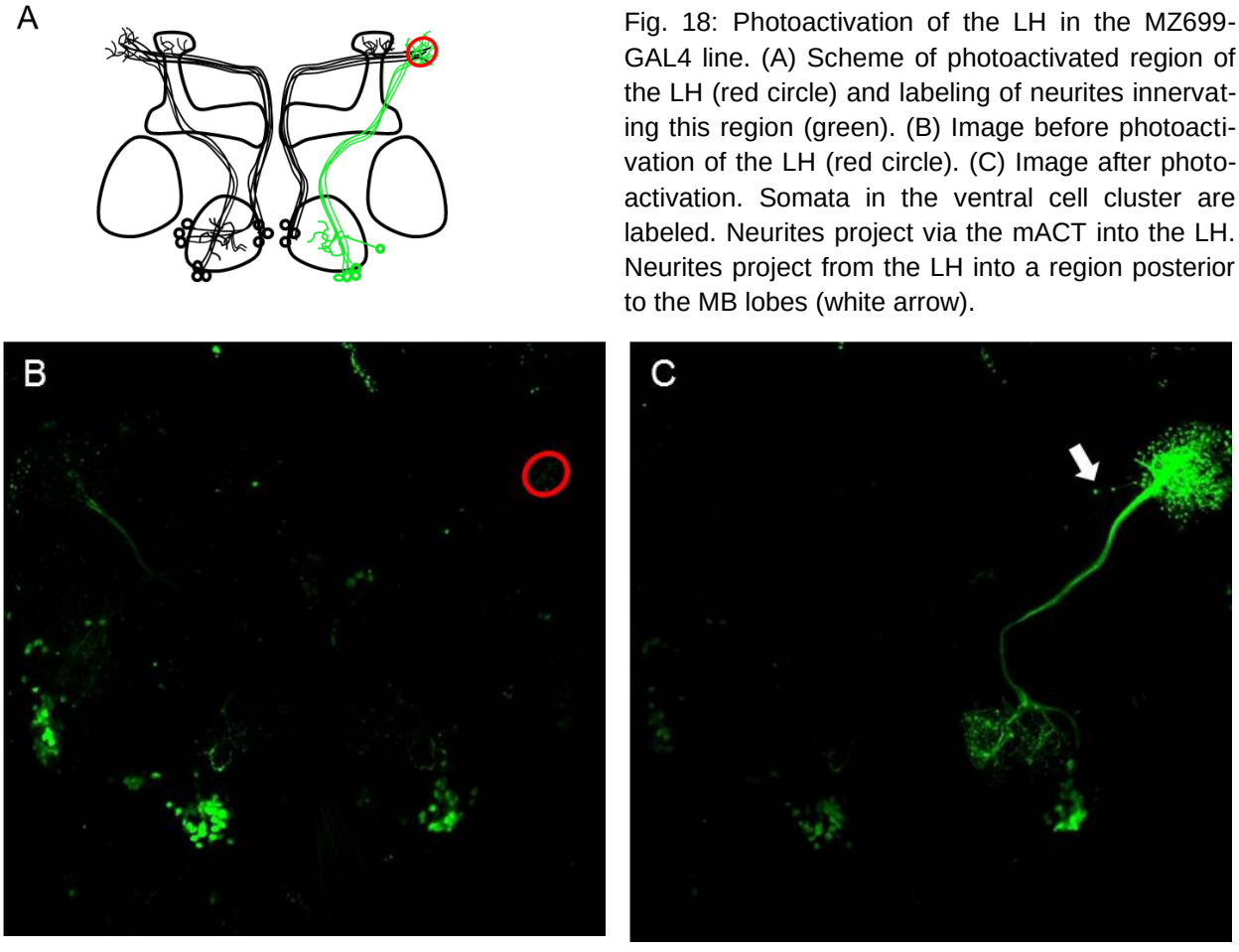

Fig. 18: Photoactivation of the LH in the MZ699-GAL4 line. (A) Scheme of photoactivated region of the LH (red circle) and labeling of neurites innervating this region (green). (B) Image before photoactivation of the LH (red circle). (C) Image after photoactivation. Somata in the ventral cell cluster are labeled. Neurites project via the mACT into the LH. Neurites project from the LH into a region posterior to the MB lobes (white arrow).

terior to the MB lobes (white arrow in Fig. 17 C). Furthermore, the MZ699-PNs that send their neurites via the mACT to the LH revealed a characteristic innervation pattern of the LH looking similar to a bottle brush. In the ventral part of the LH the labeled neurites extended their branches into the vlPr, whereas neurites in the medial side of the LH extended also to the MB calyx. The synaptic terminals were much brighter than the neurites. As has already been described for the AL above, two neurites projected from the LH to a region that is located posterior to the MB lobes (white arrow in Fig.17 C).

In order to label all MZ699-neurons, that are innervating the LH, I photoactivated a small region in the LH, where the neurites of the mACT showed their first arborizations. This revealed weaker fluorescence signals of glomeruli and somata (Fig. 18) in comparison to the results seen after photoactivation of the whole AL. Interestingly, only the two neurites projecting from the LH into a region located posterior to the MB lobes were discernible (white arrow in Fig. 18 C) and not the neurites projecting from the AL to a region posterior to the MB lobes.

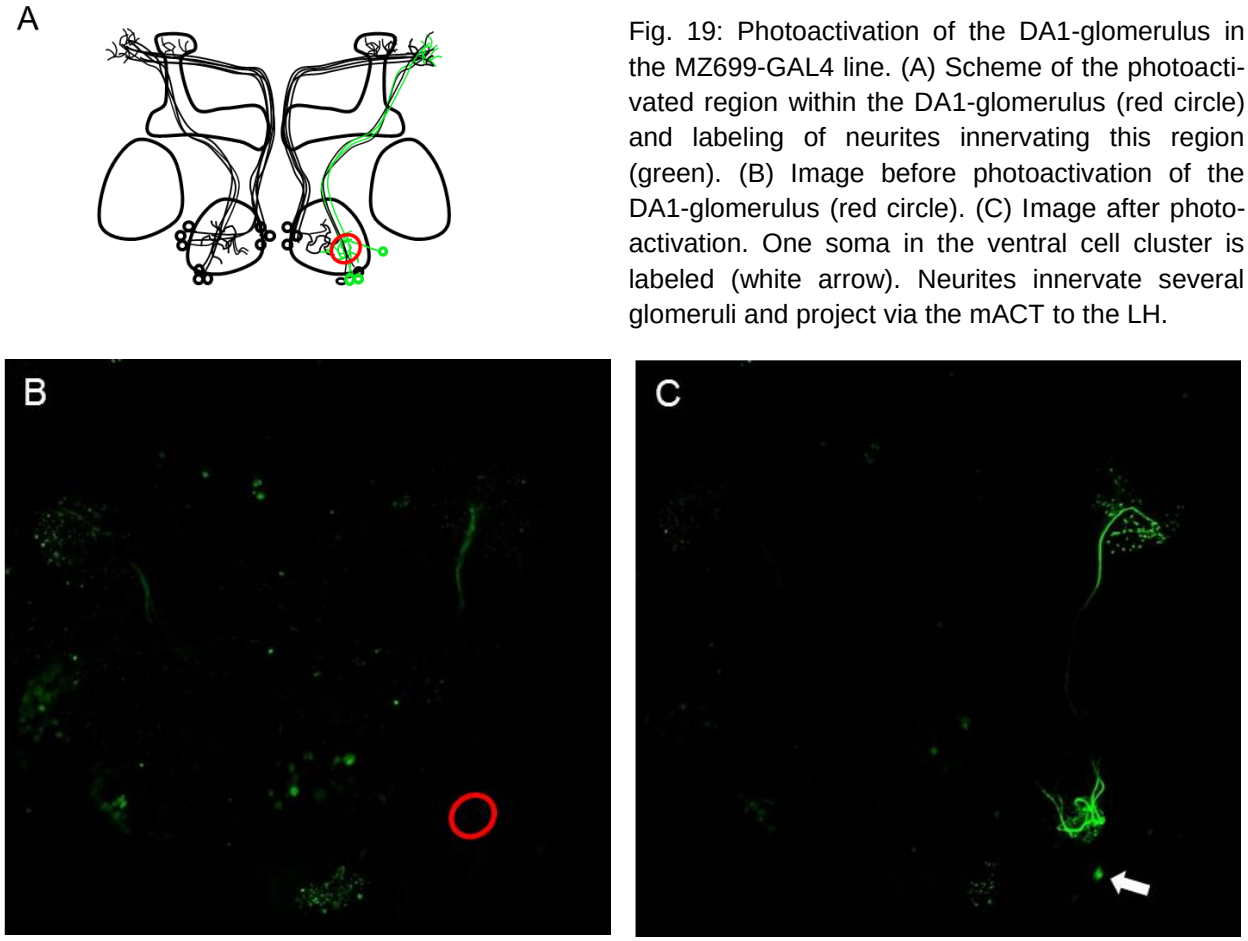

Fig. 19: Photoactivation of the DA1-glomerulus in the MZ699-GAL4 line. (A) Scheme of the photoactivated region within the DA1-glomerulus (red circle) and labeling of neurites innervating this region (green). (B) Image before photoactivation of the DA1-glomerulus (red circle). (C) Image after photoactivation. One soma in the ventral cell cluster is labeled (white arrow). Neurites innervate several glomeruli and project via the mACT to the LH.

For comparison of the innervation patterns of subsets of PNs in a single glomerulus I photoactivated the DA1-glomerulus also in the MZ699-GAL4 line. The photoactivation of DA1 (Fig. 19) showed arborizations in neighboring glomeruli, that can most likely be identified as the glomeruli DA2 and VA1. This observation supports that MZ699-PNs have multiglomerular branches. Moreover only the ventral part of the LH was innervated via the mACT by the labeled neurite. Furthermore, one soma was labeled (white arrow in Fig. 19 C), that was located in the ventral cell cluster. It could be possible that this ventral soma is the same one as has been labeled by photoactivation in the GH146-GAL4 line. However, this assumption has to be analyzed in further experiments.

To compare the innervation pattern of subsets of PNs innervating the VM2-glomerulus I photoactivated this glomerulus also in the MZ699-GAL4 line. After the photoactivation of glomerulus VM2 neurites with arborizations in neighboring glomeruli and three somata were labeled (Fig. 20). The labeled neurites innervated the LH via the mACT and showed a similar innervation pattern with labeled synaptic terminals distributed in the whole LH.

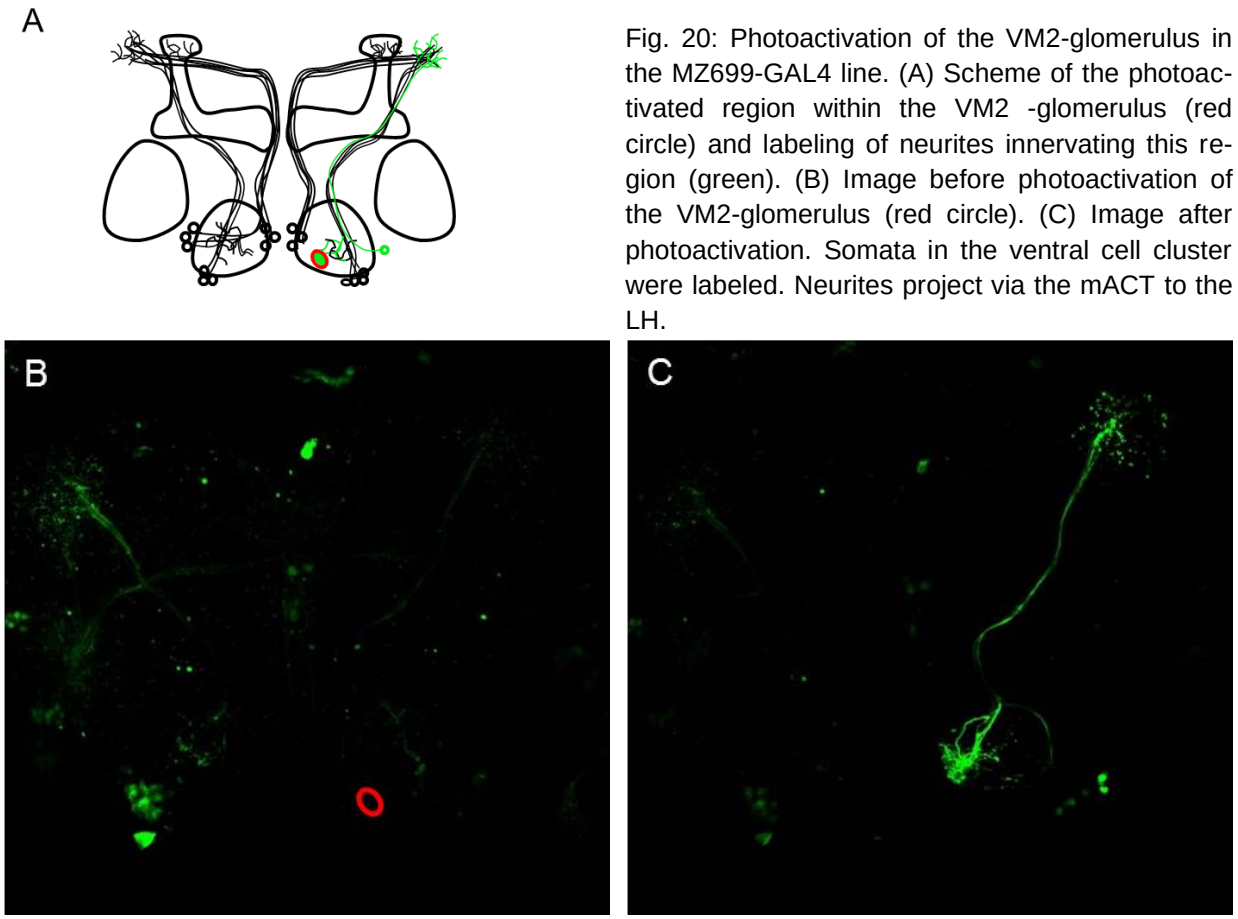

Fig. 20: Photoactivation of the VM2-glomerulus in the MZ699-GAL4 line. (A) Scheme of the photoactivated region within the VM2 -glomerulus (red circle) and labeling of neurites innervating this region (green). (B) Image before photoactivation of the VM2-glomerulus (red circle). (C) Image after photoactivation. Somata in the ventral cell cluster were labeled. Neurites project via the mACT to the LH.

The photoactivation experiments were also used to activate single somata in order to visualize single MZ699-PNs. As already described for the photoactivation of single soma in the GH146-GAL4 line in several attempts unfortunately more than one cell body was labeled. However, the labeling of single somata was successful and is represented as an example in Fig. 21. The labeled PN innervated glomeruli of the lateral side of the AL and innervated the whole LH via the mACT. Since it was very difficult to photoactivate a single PN in the MZ699-GAL4 line, the sample number is unfortunately very small and does not allow drawing conclusions regarding the general innervation patterns of single MZ699-PNs. In future experiments the innervation patterns of the remaining PNs of the ventral cell cluster needs to be analyzed in more detail.

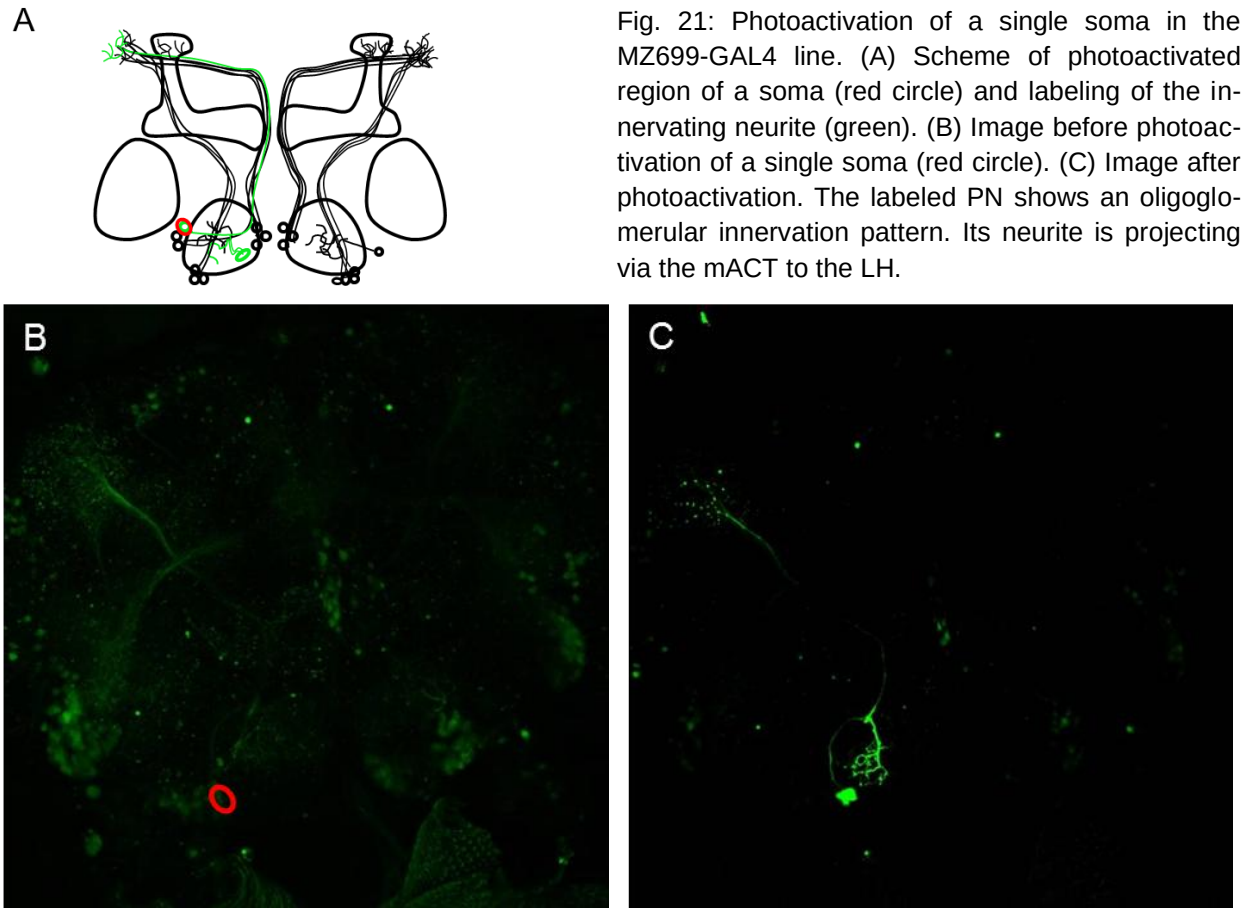

Fig. 21: Photoactivation of a single soma in the MZ699-GAL4 line. (A) Scheme of photoactivated region of a soma (red circle) and labeling of the innervating neurite (green). (B) Image before photoactivation of a single soma (red circle). (C) Image after photoactivation. The labeled PN shows an oligoglomerular innervation pattern. Its neurite is projecting via the mACT to the LH.

3.4 Comparison of the innervation patterns of GH146- and MZ699-PNs

For morphological analyses of the enhancer trap lines GH146-GAL4 and MZ699-GAL4 I used PA-GFP utilizing its potentiality of labeling distinct structures. The photoactivation experiments revealed the innervation patterns of PNs labeled by both used enhancer trap lines. Photoactivation of either the whole AL or the LH showed labeling of all PNs innervating these brain structures. Around 100 neurons of the anterodorsal, lateral and ventral cell cluster labeled by the GH146-GAL4 line innervated a subset of 32 glomeruli (V. Grabe, unpublished). Approximately four PNs in the GH146-GAL4 line projected from the AL via the mACT directly to the LH and the remaining PNs projected via the iACT to the MB calyx and then to the LH (Figures 12 & 13). The neurites of the iACT showed arborizations in the MB calyx and the whole LH appeared to be innervated. Interestingly, single neurites extended from the LH to a region posterior to the MB lobes (not shown). Around 50 PNs of the ventral cell cluster labeled in the MZ699-GAL4 line innervated a subset of 21 glomeruli (V. Grabe, unpublished) and projected from the AL via the mACT to the LH (Figures 17 & 18). Within the LH a characteristic regional innervation pattern was discernible. Interestingly, single neurites extended from the LH or rather the AL to a region posterior to the MB lobes (Figures 17 C & 18 C).

The GH146-GAL4 line showed a uniglomerular innervation pattern in the AL, which was convenient to identify single glomeruli for the photoactivation. In comparison, the MZ699-GAL4 line showed a rather mulitglomerular innervation pattern in the AL that required the DsRed-staining of the neuropil to identify single glomeruli. The photoactivation in the GH146-GAL4 line of single glomeruli, in this case DA1 and VM2 (Figures 14 & 15), revealed also an oligoglomerular innervation pattern for single neurons. In MZ699-GAL4 line the photoactivation of the two glomeruli DA1 and VM2 (Figures 19 & 20) verified the oligolgomerular innervation pattern. Since only a small number of varying single neurons were labeled by photoactivation in both GAL4 lines (Figures 16 & 21) it is not possible to compare the innervation patterns between both PN types. However, the predominant uniglomerular innervation pattern of PNs in the GH146-GAL4 line and the strictly oligoglomerular innervation pattern of PNs in the MZ699-GAL4 line is evident.

In the GH146-GAL4 line the DGI was labeled also with its cell body next to the vlPr. Photoactivation of the DGI was performed only once and revealed the innervation of the MB calyx with projections through the LH as well as arborizations to the MB lobes (data not shown).

A comparison of the size of somata labeled by the MZ699-GAL4 line and the GH146-GAL4 line revealed that the cell bodies of the three cell clusters labeled with the GH146-GAL4 line were

twice as big as the cell bodies of the ventral cell cluster labeled with the MZ699-GAL4 line. This could result in a higher number of expressed PA-GFP molecules in PNs in the GH146-GAL4 line and thus could be one reason for the higher fluorescence signal occurring before and after photoactivation in GH146 in comparison to MZ699.

During my diploma thesis I could successfully establish a protocol for the photoactivation of different olfactory PN types. However, these experiments are only the beginning of a much more detailed morphological analysis that is needed to characterize the different innervation patterns of single PNs in these GAL4 lines. Further morphological studies will reveal additional features of the analyzed PNs.

4. Discussion

The aim of this work was the analysis of putatively inhibitory PNs (Wilson & Laurent, 2005) labeled by the MZ699-GAL4 enhancer trap line in *Drosophila melanogaster*. These neurons have their cell bodies located in the ventral cell cluster of the AL. In order to determine the expressed neurotransmitter in these PNs I used immunostaining in dissected fly brains against the inhibitory neurotransmitter GABA and against the enzyme ChAT, which is producing the excitatory neurotransmitter ACh.

The morphology of MZ699-PNs was analyzed by using PA-GFP that enables labeling of distinct structures by photoactivation of PA-GFP molecules. The successful establishment of a protocol for PA-GFP expressed in neurons of the enhancer trap line MZ699 enables now to further analyze the innervation pattern in the entire fly brain of all neurons of interest.

4.1 MZ699-PNs are not exclusively GABA-positive

In recent papers (Okada *et al.*, 2009; Lai *et al.*, 2008; Enell *et al.*, 2007; Jefferis *et al.*, 2007; Wilson & Laurent, 2005; Jackson *et al.*, 1990) it has been shown that PNs of the ventral cell cluster labeled by different enhancer trap lines mainly express the inhibitory neurotransmitter GABA. In these studies different techniques as immunostaining or *in situ* hybridization were used to analyze the neurotransmitter of different olfactory neuron populations. In order to confirm the expression of GABA in PNs labeled by the MZ699-GAL4 line I used immunostaining against GABA. The same antibody was also used by Wilson & Laurent (2005), who labeled GABA-positive cells of the GH298-GAL4 line, which labels mainly local interneurons in the *Drosophila* AL.

The anti-GABA immunostaining of the MZ699-GAL4-line revealed a labeling of several cell clusters and brain structures in the entire fly brain (Fig. 9). Also some PNs of the ventral cell cluster were labeled. But in-depth analysis revealed a labeling of a much lower number of MZ699-PNs as described by Okada *et al.* (2009). Only 16 to 34 % of all MZ699-PNs showed labeling in anti-GABA immunostaining (table 2), whereas Okada *et al.* (2009) described that around 80 % of all MZ699-PNs express GABA. One reason for this strong difference could be that the use of antibodies against proteins, or in this case amino acids, detects exactly these molecules, whereas *in situ* hybridization labels the mRNA of expressed proteins. The latter method has been used by Okada *et al.* (2009) to label GAD (glutamic acid decarboxylase), the producing enzyme of

GABA. But the detection of the existence of the mRNA, which will be translated into a protein, does not necessarily mean that this protein will be consequently active, i.e. an existing GAD-protein in a neuron does not prove the synthesis of GABA in the end. Interestingly, Enell *et al.* (2007) has described a strong increase of the expression of GAD1-GAL4 with the distribution of GABA in the *Drosophila* brain. However, in this context they also showed that GAD was present in glutamatergic and in other neurons.

In order to confirm one of each result of the number of labeled MZ699-PNs further analyses using different methods are necessary to prove the existence of GABA in these neurons. One possibility is the crossing of a GAD-GAL4 line with the MZ699-GAL4 line that should reveal the expression of GAD in MZ699-PNs by co-localization. This expression of fluorescent proteins in the MZ699-neurons would overcome the non-specific labeling that might occur in *in situ* hybridization. Another possibility is the use of different antibodies against GABA or also against GAD in the MZ699-GAL4 line.

Interestingly, MZ699-PNs which showed no labeling by anti-GABA immunostaining were also not labeled by anti-ChAT immunostaining (Fig. 9 B2; N. K. Tanaka, personal communication) meaning that these neurons are neither GABAergic nor cholinergic as the majority of PNs. Further analyses are needed to identify the neurotransmitter of the remaining MZ699-PNs. Other neurotransmitter expressed in these neurons could be dopamine or serotonin, synthesized by the *Drosophila* DOPA decarboxylase (DDC; Jackson *et al.*, 1990). Also the expression of glutamic acid and a combination of neurotransmitter could be possible as it has been described by Chou *et al.* (2010) for LNs. Histamine can be excluded as a neurotransmitter in these PNs, because anti-histamine immunostaining showed only a weak labeling in the fly brain and no labeling of cell clusters around the antennal lobe at all (Pollack & Hofbauer, 1991). Several neuropeptides are expressed in *Drosophila.* A few of these has been already detected in OSNs and LNs but not yet in PNs (see review by Nässel & Winther, 2010).

4.2 Age-dependency of the number of MZ699-PNs

Immunostaining against GABA showed a strong variability in the number of GABAergic MZ699-PNs as well as in the total number of MZ699-PNs. I counted 3 to 25 (47 as an outlier) labeled GABAergic MZ699-PNs. The variability of the total number of 32 to 55 PNs (64 PNs as an outlier) of the MZ699-GAL4 line was also observed by Okada *et al.* (2009), who identified 30 to 52 MZ699-PNs. Okada *et al.* have done their experiments using 5 to 10 days old flies whereas I used 1 to 6 days old flies for my analysis. The variability of both the total number of MZ699-PNs and the number of MZ699-PNs labeled in GABA-immunostaining might depend on the age of used flies. To verify if this is in fact due to the different age I performed immunostainings against GABA using (female) flies of the enhancer trap line MZ699 with an increasing age beginning with 5 h up to 15 days after eclosion. Counting the total number of MZ699-PNs as well as the number of GABAergic MZ699-PNs revealed indeed an increase depending on the age of flies. The total number of PNs varied at all ages but showed a median increase from 38 up to 50 PNs (table 1, Fig. 10). GABAergic PNs showed a doubling in the number of labeled cells from 6 to 17 in median.

Where does this increase in cell number derive from? This increase in labeling could possibly be due to an accumulation of GFP- and/or GABA-molecules expressed within these neurons with rising age and thus leading to an increase in the signal-to-noise ratio of the GFP detection. Another possibility could be that the increasing number of GABAergic PNs is an indication for the plasticity of the nervous system, which was for example described for the number of KC fibers depending on the living conditions of flies or the larvae (Technau, 1984; Balling *et al.*, 1987; Heisenberg *et al.*, 1995). In this context the production of GABA by GAD could get stronger with increasing age. A deriving of newborn PNs from neuroblasts can be excluded since neurogenesis has not been observed in the olfactory system of adult *Drosophila* in contrast to other arthropods.

The increase of labeled PNs (or other brain structures) depending on the age of flies has to be taken into account when comparing observations described in different papers; for example, Ito *et al.* (1997) used 10 days old flies and Okada *et al.* (2009) 5 to 10 days old ones in morphological analyses, Wilson & Laurent (2005) used 3 to 10 days old flies for electrophysiological analyses, and the lab of S. Sigrist usually using 30 days old flies for the detection of synaptic proteins (K. Liu, personal communication).

4.3 PA-GFP successfully established in MZ699-PNs

For morphological analyses of PNs in the enhancer trap line MZ699 PA-GFP was expressed in this GAL4-line to label and analyze single neurons. But before analyzing MZ699-PNs the functionality of the system and the expression of the C3PA-GFP (Ruta *et al.*, 2010) in olfactory PNs was tested in flies carrying the genotype +; GH146-GAL4; UAS-C3PA, because Datta *et al.* (2008; also Ruta *et al.*, 2010) described a successful protocol for photoactivation of single neurons using the GH146-enhancer trap line. Therefore, I used these flies to check different scanning and excitation parameters in order to establish a protocol for the actual experiments using the MZ699-GAL4 line. Several times the parameters of the protocol had to be modified and adapted since, in comparison to the GH146-GAL4 line, the use of the photoactivation protocol in MZ699-GAL4 line revealed more difficulties: e.g. weaker pre- and post-activation signals as well as the effect of “cooking” neurons (Fig. 8). The “cooking” could be fortunately terminated by the use of light of 760-nm wavelength in a continuous light exposure mode. The weaker pre- and postactivation signal in the MZ699-GAL4 line compared to the GH146-GAL4 line could derive from a lower expression level of PA-GFP in these neurons due to two reasons: first, the somata of MZ699-PNs are much smaller than those of the GH146-PNs. Second the promoter of the MZ699-GAL4 line could be less strong and hence the expression level could be reduced. Both reasons would result in a lower accumulation of PA-GFP molecules and thus a weaker PA-GFP labeling of these PNs.

However, despite the described difficulties a protocol could be established for PA-GFP in the MZ699-line which resulted in a strong fluorescence increase after photoactivation in comparison to the non-activated structures and revealed characteristic innervation patterns in the AL and the LH. Jefferis *et al.* (2007) and Marin *et al.* (2002) who studied in detail the morphology of single PNs labeled by the GH146-line have described that these PNs innervate the LH in a complex and characteristic way which cannot be seen in the MB calyx. Interestingly I could find very similar innervation patterns for the MZ699-PNs. Moreover, Marin *et al.* (2002) revealed in 3D-reconstructions the individual differences in the innervation pattern of single PNs which are showing a similar two-dimensional innervation pattern. Thus, in further experiments 3D-reconstructions of labeled MZ699-PNs need to be performed to analyze individual differences of MZ699-PNs showing a similar innervation pattern (e.g. neurons innervating the VM2-glomerulus; Fig. 20).

During my diploma thesis I used only young flies (1 to 3 days old) for the photoactivation experiments. In consideration of the increasing number of PNs due to the age of the fly revealed by immunostaining experiments the photoactivation experiments should be repeated with flies older than three days to analyze a possible variance in the innervation patterns of MZ699-PNs.

4.4 MZ699-PNs are multiglomerular

The analysis of the morphology of MZ699-PNs by using photoactivation of distinct brain structures, e.g. labeling of PNs innervating only the glomeruli DA1 and VM2, revealed a multiglomerular innervation pattern in the AL. Interestingly, photoactivation of the DA1 glomerulus resulted for both enhancer trap lines in the labeling of a single PN of the ventral cell cluster (Figures 14 & 19). At first view these two PNs labeled by the two GAL4 lines appeared to be identical. However, Lai *et al.* (2008) revealed that the enhancer trap lines GH146 and MZ699 show no overlap in the labeling of PNs of the ventral cell cluster. Thus, to get a comprehensive map of the neurons innervating a distinct glomerulus different GAL4-lines have to be used in further analyses. As it has been observed for the photoactivation of single glomeruli, the labeling of single neurons of the ventral cell cluster in the MZ699-GAL4 line revealed also a multiglomerular innervation in the AL (Fig. 21). Interestingly, Lai *et al.* (2008) have also described a uniglomerular innervation pattern for PNs belonging to the ventral cell cluster, which could not be observed here. In accordance with the data shown here, Marin *et al.* (2002) described one PN of the ventral cell cluster in the GH146-GAL4 line that innervated (nearly) the whole AL. In further analyses using the established photoactivation protocol these observations have to be verified for both the MZ699-GAL4 line and the GH146-GAL4 line by labeling a variety of individual PNs.

A map of the innervated glomeruli in the MZ699-GAL4 line, which has been generated by V. Grabe (unpublished; not shown) can now be used as a template for the analyses of further glomeruli. Furthermore, expanding the present experiments by the use of a neuropil marker as nc82-immunostaining after the photoactivation of single glomeruli or even single neurons would enable a detailed 3D-reconstruction of the innervation pattern in the AL and the LH. This would also allow the identification of all innervated glomeruli of the labeled neuron(s) as well as a more detailed analysis of the innervation pattern in the higher brain areas.

4.5 GH146-PNs and MZ699-PNs leave the AL through different pathways

As has already been described by Stocker *et al.* (1997) PNs labeled by the GH146-GAL4 line project via the iACT to the MB calyx and to the LH. Only a few PNs project via the mACT directly to the LH. In comparison, PNs of the MZ699-GAL4 line project exclusively via the mACT to the LH and bypass the MB calyx region (Ito *et al.*, 1997). The PNs of the iACT represent the main connection between the AL and the MB, which is the higher processing center for short and long term memory in odor discrimination tasks (see review by Heisenberg, 1998). Within the MB calyx the PNs form synapses on so-called Kenyon-cells (KC). Heisenberg *et al.* (1985) showed that the deficiency of > 90 % of KCs let flies still behave normally including their innate response to attractive or aversive odors. However, flies are not able anymore to perform olfactory associative learning tasks. In another study de Belle *et al.* (1994) could show that the ablation of the whole MB leads to an almost completely loss of aversive associative learning by pairing an odor with an electric-shock. Interestingly, the ablation of the MB has no effect onto the behavioral response to either pure or diluted odors. In conclusion one can assume that other aspects of olfaction, like the innate response to odors, are processed in further brain areas like the LH, indicated by the extension of PNs in this brain region. This assumption is indeed supported by a study by Heimbeck *et al.* (2001) who have blocked the synaptic transmission in PNs by expressing tetanus toxin in these neurons. Their results imply that the direct PN-to-LH pathway is necessary and sufficient to process experience-independent behaviors.

In summary, the MB is necessary for olfactory learning as well as memory tasks while the LH might be necessary for innate olfactory responses. Consequential, MZ699-PNs which innervate directly the LH could transfer the information about aversive or attractive odors to enable a rapid behavioral response. However, since only a few glomeruli (about one third) are innervated by PNs of the ventral cell cluster, the combinatorial code for attractive or aversive odors would be somehow limited. On the other hand, the multiglomerular innervation patterns of these PNs would allow collecting the odor information of nearly every glomerulus in the fly AL. Moreover this complex innervations pattern could also imply an inherent pattern of glomeruli that have to be activated to drive an innate response in the LH. The role of the LH for the coding of odors and/or innate responses has to be analyzed in further experiments, e.g. by analyzing the functional response patterns of MZ699-PNs to odors within the innervated glomeruli and LH.

5. References

- Adams MD, *et al.* (2000); The Genome Sequence of *Drosophila melanogaster*; Science, 287: 2185-2195

- Bachmann A & Knust E (2008); The Use of P-Element Transposons to Generate Transgenic Flies; Methods in Molecular Biology, 420: 61-77

- Balling A, Technau GM, Heisenberg M (1987); Are the structural changes in adult *Drosophila* mushroom bodies memory traces? Studies on biochemical learning mutants; Journal of Neurogenetics, 4: 65-73

- Benton R, Sachse S, Michnick SW, Vosshall LB (2006); Atypical Membrane Topology and Heteromeric Function of *Drosophila* Odorant Receptors *In Vivo*; PLoS, 4(2): 240-257

- Benton R, Vannice KS, Gomez-Diaz C, Vosshall LB (2009); Variant ionotropic glutamate receptors as chemosensory receptors in Drosophila; Cell, 136: 149-162

- Brand AH & Perrimon N (1993); Targeted gene expression as a means of altering cell fates and generating dominant phenotypes; Development, 118: 401-415

- Cavener DR (1987); Comparison of the consensus sequence flanking translational start sites in *Drosophila* and vertebrates; Nucleic Acids Research, 15 (4): 1353-1361

- Chou Y-H, Spletter ML, Yaksi E, Leong JCS, Wilson RI, Luo L (2010); Diversity and wiring variability of olfactory local interneurons in the *Drosophila* antennal lobe; Nature Neuroscience, 13 (4): 439-449

- Clyne PJ, Warr CG, Freeman MR, Lessing D, Kim J, Carlson JR (1999); A Novel Family of Divergent Seven-Transmembrane Proteins: Candidate Odorant Receptors in *Drosophila*; Neuron, 22: 327-338

- Couto A, Alenius M, Dickson BJ (2005); Molecular, Anatomical, and Functional Organization of the *Drosophila* Olfactory System; Current Biology, 15: 1535-1547

- Datta SR, Vasconcelos ML, Ruta V, Luo S, Wong A, Demir E, Flores J, Balonze K, Dickson BJ, Axel R (2008); The *Drosophila* pheromone cVA activates a sexually dimorphic neural circuit; Nature, 452 (7186): 473-477

- de Belle SJ, Heisenberg M (1994); Associative Odor Learning in *Drosophila* Abolished by Chemical Ablation of Mushroom Bodies; Science, 263: 692-695

- Denk W, Strickler JH, Webb WW (1990); Two-Photon Laser Scanning Fluorescence Microscopy; Science, 248 (4951): 73-76

- DiAntonio A, Burgess RW, Chin AC, Deitcher DL, Scheller RH, Schwarz TL (1993); Identification and Characterization of *Drosophila* Genes for Synaptic Vesicle Proteins; Journal of Neuroscience, 73 (11): 4924-4935

- Dobritsa AA, van der Goes van Naters W, Warr CG, Steinbrecht RA, Carlson JR (2003); Integrating the Molecular and Cellular Basis of Odor Coding in the *Drosophila* Antenna; Neuron, 37: 827-841

- Elliott DA & Brand AH (2008); The GAL4 System - A Versatile System for the Expression of Genes; Methods in Molecular Biology, 420: 79-95

- Enell L, Hamasaka Y, Kolodziejczyk A, Nässel DR (2007); Gamma-Aminobutyric Acid (GABA) Signaling Components in *Drosophila*: Immunocytochemical Localization of $GABA_B$ Receptors in Relation to the GABAA Receptor Subunit RDL and a Vesicular GAB_A Transporter; Journal of Comparative Neurology, 505: 18-31

- Fishilevich E & Vosshall LB (2005); Genetic and Functional Subdivision of the *Drosophila* Antennal Lobe; Current Biology, 15: 1548-1553

- Gao Q & Chess A (1999); Identification of Candidate *Drosophila* Olfactory Receptors from Genomic DNA Sequence; Genomics, 60: 31-39

- Goldman AL, van der Goes van Naters W, Lessing D, Warr CG, Carlson JR (2005); Co-expression of Two Functional Odor Receptors in One Neuron; Neuron, 45: 661-666

- Hansson BS, Knaden M, Sachse S, Stensmyr MC, Wicher D (2010); Towards plant-odor-related olfactory neuroethology in *Drosophila*; Chemoecology, 20 (2): 51-61

- Heimbeck G, Bugnon V, Gendre N, Keller A, Stocker RF (2001); A central neural circuit for experience-independent olfactory and courtship behavior in *Drosophila melanogaster*; PNAS, 98 (26): 15336-16341

- Heisenberg, M, Borst A, Wagner S, Byers D (1985); *Drosophila* mushroom body mutants are deficient in olfactory learning; Journal of Neurogenetics, 2: 1-30

- Heisenberg M, Heusipp M, Wanke C (1995); Structural Plasticity in the *Drosophila* Brain; The Journal of Neuroscience, 75 (3): 1951-1960

- Heisenberg M (1998); What Do the Mushroom Bodies Do for the Insect Brain? An Introduction; Learning & Memory, 5: 1–10

- Hildebrand JG & Shepherd GM (1997); MECHANISMS OF OLFACTORY DISCRIMINATION: Converging Evidence for Common Principles Across Phyla; Annual Reviews in Neuroscience, 20: 595-631

- Hummel T & Klämbt C (2008); P-Element Mutagenesis; Methods in Molecular Biology, 420: 97-117

- Ignell R, Root CM, Birsec RT, Wang JW, Nässel DR, Winther ÅME (2009); Presynaptic peptidergic modulation of olfactory receptor neurons in *Drosophila*; PNAS, 106 (31): 13070-13075

- Ito K, Sass H, Urban J, Hofbauer A, Schneuwly S (1997); GAL4-responsive UAS-tau as a tool for studying the anatomy and development of the *Drosophila* central nervous system; Cell Tissue Research, 290: 1-10

- Jackson FR, Newby LM, Kulkarni SJ (1990); *Drosophila* GABAergic Systems: Sequence and *Expression* of Glutamic Acid Decarboxylase; Journal of Neurochemistry, 54 (3): 1068-1078

- Jefferis GSXE, Potter CJ, Chan AM, Marin EC, Rohlfing T, Maurer CR Jr., Luo L (2007); Comprehensive Mapsof *Drosophila* Higher Olfactory Centers: Spatially Segregated Fruit and Pheromone Representation; Cell, 128: 1187-1203

- Lai S-L, Awasaki T, Ito K, Lee T (2008); Clonal analysis of *Drosophila* antennal lobe neurons: diverse neuronal architectures in the lateral neuroblast lineage; Development, 135: 2883-2893

- Laissue PP, Reiter C, Hiesinger PR, Halter S, Fischbach KF, Stocker RF (1999); Three-Dimensional Reconstruction of the Antennal Lobe in *Drosophila melanogaster*; Journal of Comparative Neurology, 405: 543-552

- Larsson MC, Domingos AI, Jones WD, Chiappe ME, Amrein H, Vosshall LB (2004); Or83b Encodes a Broadly Expressed Odorant Receptor Essential for *Drosophila* Olfaction; Neuron, 43: 703-714

- Liang L & Luo L (2010); The olfactory circuit of the fruit fly *Drosophila melanogaster;* Science China Life Science, 53: 472-484,

- Luo L, Callaway EM, Svoboda K (2008); Genetic Dissection of Neural Circuits; Neuron, 57 (5): 634-660

- Marin EC, Jefferis GSXE, Komiyama T, Zhu H, Luo L (2002); Representation of the Glomerular Olfactory Map in the *Drosophila* Brain; Cell, 109: 243-255

- Matz MV, Fradkov AF, Labas YA, Savitsky AP, Zaraisky AG, Markelov ML, Lukyanov SA (1999); Fluorescent proteins from nonbioluminescent Anthozoa species; Nature Biotechnology, 17: 969-973

- Nässel DR & Winther ÅME (2010); *Drosophila* neuropeptides in regulation of physiology and behavior; Progress in Neurobiology, 92: 42-104

- Nakai J, Ohkura M, Imoto K (2001); A high signal-to-noise Ca^{2+} probe composed of a single green fluorescent protein; Nature Biotechnology, 19: 137-141

- Okada R, Awasaki T, Ito K (2009); Gamma-Aminobutyric Acid (GABA)-Mediated Neural Connections in the *Drosophila* Antennal Lobe; The Journal of Comparative Neurology, 514: 74-91

- Patterson GH & Lippincott-Schwartz J (2002); A Photoactivatable GFP for Selective Photolabeling of Proteins and Cells; Science, 297: 1873-1877

- Pollack I, Hofbauer A (1991); Histamine-like immunoreactivity in the visual system and brain of *Drosophila melanogaster*; Cell Tissue Research, 266: 391-398

- Robertson HM, Warr CG, Carlson JR (2003); Molecular evolution of the insect chemoreceptor gene superfamily in *Drosophila melanogaster*; PNAS, 100: 14537-14542

- Ruta V, Datta SR, Vasconcelos ML, Freeland J, Looger LL, Axel R (2010); A dimorphic pheromone circuit in *Drosophila* from sensory input to descending output; Nature, 468: 686-690

- Sargsyan V, Getahun MN, Llanos SL, Olsson SB, Hansson BS, Wicher D (2011); Phosphorylation via PKC regulates the function of the *Drosophila* odorant co-receptor; Frontiers in Cellular Neuroscience, 5: 1-8

- Sato K, Pellegrino M, Nakagawa T, Nakagawa T, Vosshall LB, Touhara K (2008) Insect olfactory receptors are heteromeric ligand-gated ion channels; Nature, 452: 1002-1006

- Seki Y, Rybak J, Wicher D, Sachse S, Hansson BS (2010); Morphological and physiological characterization of excitatory and inhibitory local interneurons in the *Drosophila* antennal lobe; Journal of Neurophysiology, 104 (2):1007-1019

- Shanbhag SR, Müller B, Steinbrecht RA (1999); Atlas of olfactory organs of *Drosophila melanogaster* 1. Types, external organization, innervation and distribution of olfactory sensilla; International Journal of Insect Morphology and Embryology, 28: 377-397

- Shang Y, Claridge-Chang A, Sjulson L, Pypaert M, Miesenböck G (2007); Excitatory Local Circuits and Their Implications for Olfactory Processing in the Fly Antennal Lobe; Cell, 128: 601-612

- Stocker RF, Lienhard MC, Borst A, Fischbach K-F (1990); Neuronal architecture of the antennal lobe in *Drosophila melanogaster*; Cell and Tissue Research, 262: 9-34

- Stocker RF (1994); The organization of the chemosensory system in *Drosophila melanogaster*: a review; Cell Tissue Research, 275: 3-26

- Stocker RF, Heimbeck G, Gendre N, de Belle S (1997); Neuroblast Ablation in *Drosophila* P[GAL4] Lines Reveals Origins of Olfactory Interneurons; Journal of Neurobiology, 32 (5): 443-456

- Stökl J, Strutz A, Dafni A,Svatos A, Doubsky J, Knaden M, Sachse S, Hansson BS, Stensmyr MC (2010); A Deceptive Pollination System Targeting Drosophilids through Olfactory Mimicry of Yeast; Current Biology, 20: 1846-1852

- Su C-Y, Menuz K, Carlson JR (2009); Olfactory Perception: Receptors, Cells, and Circuits; Cell, 139 (1): 45-59

- Technau GM (1984); Fiber Number in the Mushroom Bodies of Adult *Drosophila melanogaster* depends on Age, Sex and Experience; Journal of Neurogenetics, 1: 113-126

- van Thor JJ (2009); Photoreactions and dynamics of the green fluorescent protein; Chemical Society Review, 38: 2935-2950

- Vosshall LB, Amrein H, Morozov PS, Rzhetsky A, Axel R (1999); A Spatial Map of Olfactory Receptor Expression in the *Drosophila* Antenna; Cell, 96: 725-736

- Vosshall LB, Wong AM, Axel R (2000); An Olfactory Sensory Map in the Fly Brain; Cell, 102: 147-159

- Wicher D, Schafer R, Bauernfeind R, Stensmyr MC, Heller R, Heinemann SH, Hansson BS (2008); *Drosophila* odorant receptors are both ligand-gated and cyclic-nucleotide-activated cation channels; Nature, 452: 1007-1011

- Wilson RI, Turner GC, Laurent G (2004); Transformation of Olfactory Representations in the *Drosophila* Antennal Lobe; Science, 303 (5656): 366-370

- Wilson RI & Laurent G (2005); Role of GABAergic Inhibition in Shaping Odor-Evoked Spatiotemporal Patterns in the *Drosophila* Antennal Lobe; Journal of Neuroscience, 25 (40): 9069-9079

- Wong AM, Wang JW, Axel R (2002); Spatial Representation of the Glomerular Map in the *Drosophila* Protocerebrum; Cell, 109: 229-241

- Wu JS & Luo L (2006); A protocol for dissecting *Drosophila melanogaster* brains for live imaging or immunostaining; Nature Protocols, 1 (4): 2110-2115.

- Xu PX, Atkinson R, Jones DNM, Smith DP (2005); *Drosophila* OBP LUSH Is Required for Activity of Pheromone-Sensitive Neurons; Neuron, 45: 193-200

- Yao K-M, Samson ML, Reeves R, White K (1993); Gene *elav* of *Drosophila melanogaster:* A Prototype for Neuronal-Specific RNA Binding Protein Gene Family That Is Conserved in Flies and Humans; Journal of Neurobiology, 24 (6): 723-739

6. Acknowledgements

First of all I thank Prof. Dr. Bill S. Hansson for giving me the opportunity to accomplish my work at the Max Planck Institute for Chemical Ecology.

Further I want to thank Dr. Silke Sachse for enhancing my knowledge to olfaction and supporting my work on every level.

Especially I want to thank Antonia Strutz and Veit Grabe for the introduction to the 2-photon laser scanning microscopy as well as for their help and critical advices during my diploma thesis.

For the introduction into immunohistology and dissection techniques during my student assistance I want to thank Yoichi Seki, since this was very helpful during my diploma thesis.

Also I want to thank all “Hanssons” for their relief and the discussions, and exceptionally for making the work in this department such enjoyable.

Finally, I thank my family and Mathias Herrmann for their support at all times during my study and especially during my diploma thesis.

7. Declaration of original authorship

I hereby declare that the work submitted is my own and that all passages and ideas that are not mine have been fully and properly acknowledged.

Jena, 10/06/2011 ……..

8. Appendix

Table: Counted numbers of PNs in the ventral cell cluster of MZ699-GAL4 line and number of co-labeled GABAergic PNs. Different colors code the age of dissected female flies. Only data highlighted by color were used for analyses. Non-colored data showed evidence of damage of the cell clusters.

Animal	Age	PNs		GABAergic PNs	
GFP MZ699 110510_1	0	38	38	5	5
GFP MZ699 110510_ 2	0	36	35	6	6
110510 4	0	38	39	7	7
GFP 1108006_1	0	41	41	7	10
110806_2	0	41	41	6	11
GC MZ699 110510_ 3	0	43	32	12	6
110510 5	0	-	30	-	6
110806_1	0	38	38	5	6
110806_4	0	-	-	-	-
110808_1(2)	2	40	38	6	8
110808_3(2)	2	36	35	8	6
110808_4(2)	2	38	36	10	8
110808_6(2)	2	45	47	13	7
110808_7(2)	2	48	45	17	13
110810_2(5)	5	38	38	8	9
MZ699_GABA_110805	6	35	39	10	10
110808_1(8)	8	49	-	15	-
110808_2(8)	8	50	-	16	-
110808_2(9)	9	51	29	11	4
110808_3(9)	9	47	50	11	9
110808_4(9)	9	50	46	8	8
110808_5(9)	9	64	46	25	14
110808_1(11)	11	40	46	12	18
110815_3(11)	11	51	-	11	-
110815_6(11)	11	-	48	-	12
110819_1(11)	11	48	49	18	16
110819_4(11)	11	48	52	16	16
110819_2(12)	12	46	55	18	15
110819_3(12)	12	51	54	9	15
110819_4(12)	12	48	-	12	-
110817_3(13)	13	54	55	12	17
110817_7(13)	13	49	55	18	19
110817_9(13)	13	49	50	17	18
110815_3(14)	14	42	43	6	10
110815_6(14)	14	27	50	4	7
GFP MZ699 110413 Tier 2	2-3	45	41	6	8

GFP MZ699 110413 Tier 3	2-3	42	42	8	9
GFP MZ699 110413 Tier 4	2-3	45	45	4	3
GFP MZ699 110211 Tier 1	1-4	37	38	12	11
GC MZ699 110211 Tier 3	1-4	47	53	15	15
GC MZ699 110308 Tier 3	3-4	-	-	-	-
GFP MZ699 110118 Tier 4	3-6 d	59	54	17	7
GFP MZ699 110120 Tier 4	3-6 d	49	44	19	17
GC MZ699 110118 Tier 3	3-6	45	46	16	14
GC MZ699 110120 Tier 3	3-6	-	37	-	8
GFP MZ699 110315 Tier 1	4-6	33	-	3?	-
GFP MZ699 110316 Tier 2	4-6	40	37	6	6
GFP MZ699 110316 Tier 3	4-6	-	-	-	-
GFP MZ699 110316 Tier 7	4-6	46	45	5	4
GC MZ699 110214Tier 1	4-6	61	58	34	47
GC MZ699 110315 Tier 3	4-6	43	53	10	13
GC MZ699 110329Tier 3	1-7	22	-	8	-
GFP MZ699 110218 Tier 4	6-9	43	46	7	9
GFP MZ699 110401 Tier 2	7-9	37	37	8	10
GFP MZ699 110401 Tier 3	7-9	43	46	10	10
GFP MZ699 110401 Tier 4	7-9	-	34	-	11
GFP MZ699 110401 Tier 5	7-9	39	39	12	11
GFP MZ699 110401 Tier 6	7-9	47	44	14	11
GC MZ699 110401Tier 7	7-9	28	18	6	-
GC MZ699 110215 Tier 1	11-13	53	52	36	40
GFP MZ699 110415 Tier 1	11-15	39	39	5	9
GFP MZ699 110415 Tier 6	11-15	46	-	7	-
GC MZ699 110415 Tier 1	11-15	-	-	-	-
GC MZ699 110415 Tier 2	11-15	-	-	-	-